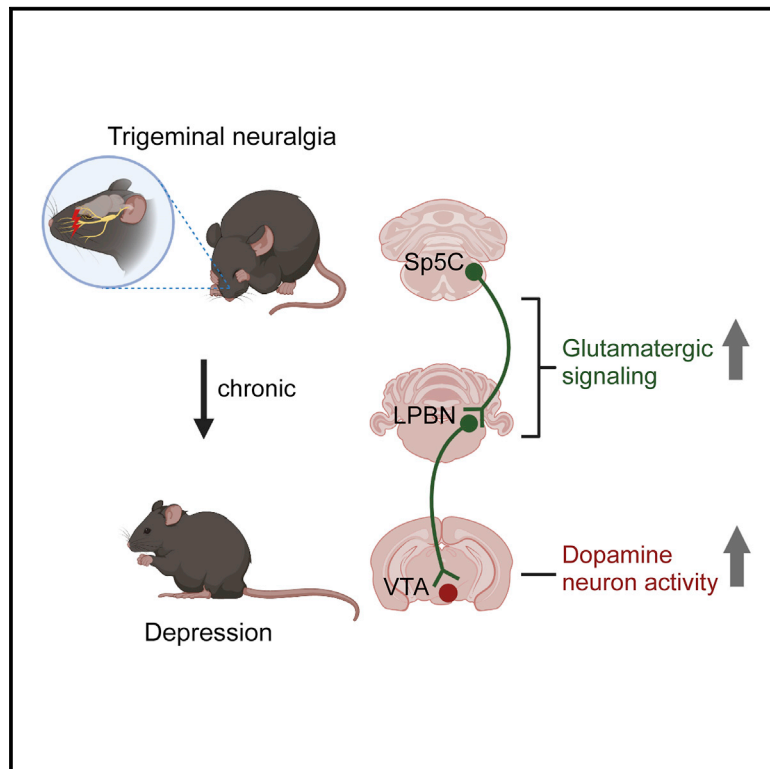# Activation of parabrachial nucleus - ventral tegmental area pathway underlies the comorbid depression in chronic neuropathic pain in mice

Graphical abstract

Authors

Ludi Zhang, Jing Wang, Chenxu Niu, ..., Nikita Gamper, Xiaona Du, Hailin Zhang

Correspondence

zhanghl@hebmu.edu.cn

In brief

Zhang et al. show that a chronic trigeminal neuralgia leads to depression, which is caused by increased activity of dopamine neurons in the midbrain. The neuronal circuits linking the spinal trigeminal subnucleus caudalis, the lateral parabrachial nucleus, and the ventral tegmental area underlie this increased activity of dopamine neurons.

Highlights

- Chronic neuropathic pain induces depression-like behaviors

- Depression behaviors are related to increased activity of VTA DA neurons

- Direct glutamatergic projections link Sp5C-LPBN-VTA

- Activation of Sp5C-LPBN-VTA leads to increased DA neuron firing and depression

Cell Reports

Article

Activation of parabrachial nucleus - ventral tegmental area pathway underlies the comorbid depression in chronic neuropathic pain in mice

Ludi Zhang,[1] Jing Wang,[1,2] Chenxu Niu,[1] Yu Zhang,[1] Tiantian Zhu,[1] Dongyang Huang,[1] Jing Ma,[1] Hui Sun,[1,3] Nikita Gamper,[1,4] Xiaona Du,[1] and Hailin Zhang[1,5,*]

[1]Department of Pharmacology, The Key Laboratory of Neural and Vascular Biology, Ministry of Education, The Key Laboratory of New Drug Pharmacology and Toxicology, Hebei Medical University, Shijiazhuang, Hebei 050017, China
[2]Department of Pharmacochemistry, Hebei University of Chinese Medicine, Shijiazhuang, Hebei 050091, China
[3]Department of Physiology, Binzhou Medical University, YanTai, Shandong 264003, China
[4]School of Biomedical Sciences, Faculty of Biological Sciences, University of Leeds, Leeds LS2 9JT, UK
[5]Lead contact
*Correspondence: zhanghl@hebmu.edu.cn
https://doi.org/10.1016/j.celrep.2021.109936

SUMMARY

Depression symptoms are often found in patients suffering from chronic pain, a phenomenon that is yet to be understood mechanistically. Here, we systematically investigate the cellular mechanisms and circuits underlying the chronic-pain-induced depression behavior. We show that the development of chronic pain is accompanied by depressive-like behaviors in a mouse model of trigeminal neuralgia. In parallel, we observe increased activity of the dopaminergic (DA) neuron in the midbrain ventral tegmental area (VTA), and inhibition of this elevated VTA DA neuron activity reverses the behavioral manifestations of depression. Further studies establish a pathway of glutamatergic projections from the spinal trigeminal subnucleus caudalis (Sp5C) to the lateral parabrachial nucleus (LPBN) and then to the VTA. These glutamatergic projections form a direct circuit that controls the development of the depression-like behavior under the state of the chronic neuropathic pain.

INTRODUCTION

The coexistence of pain and depression is a phenomenon well recognized clinically (Gallagher and Verma, 1999; Bair et al., 2003; Simon et al., 1999; Arnow et al., 2006). Symptoms of pain and depression respond to similar drug treatments, exacerbate each other, and share biological pathways and neurotransmitters (Blier and Abbott, 2001; Cohen et al., 2012), which may often complicate clinical diagnosis and treatment (Gallagher and Verma, 1999; Bair et al., 2003; Simon et al., 1999). Thus, a key to effective treatments of comorbid pain and depression lies in the understanding of the neurological, structural, and functional basis of this comorbidity. However, our understanding of how these distinct neurological phenomena are related on a neural circuit level is only beginning to emerge (Zhou et al., 2019).

Dopaminergic (DA) neurons in the midbrain ventral tegmental area (VTA) were identified to encode reward prediction error (Cohen et al., 2012). Recent studies indicate that DA neurons in the reward circuit of the VTA play a crucial role in the development of depression and represent a major target of antidepressant drugs (Lammel et al., 2014; Friedman et al., 2008; Krishnan et al., 2007; Yadid and Friedman, 2008; Chaudhury et al., 2013). For example, increased spontaneous and burst firing of the VTA DA neurons was found in some rodent models of depression

(Friedman et al., 2008; Krishnan et al., 2007); moreover, antidepressant fluoxetine can revert this increased activity (Cao et al., 2010). These observations suggest that the high firing activity of the VTA DA neurons is a salient characteristic of depression (Krishnan et al., 2007; Chaudhury et al., 2013) and that dysfunctions of the DA circuit of the VTA DA are responsible for depression conditions (Chaudhury et al., 2013; Tye et al., 2013). Interestingly, recent work also shows that activity of VTA DA neurons regulates neuropathic pain (Huang et al., 2020). Thus, gabapentin reversed nerve-injury-related depression behavior and increased activity of VTA DA neurons (Fu et al., 2018). However, it is still unknown if the VTA DA neurons are involved in comorbid depression in chronic pain.

The firing activity of the VTA DA neurons is regulated by the input projections; moreover, the glutamatergic input appears to be necessary for the burst firing activity of the VTA DA neurons (Overton and Clark, 1997; Zweifel et al., 2009; Omelchenko et al., 2009; Dobi et al., 2010). Prominent brain regions that receive or send the VTA projections include nucleus accumbens (NAc), dorsal raphe nucleus (DRN), medium prefrontal cortex (mPFC), and lateral habenula (LHb). These networks of circuits have been implicated in depression behaviors (Gunaydin et al., 2014; Zhang et al., 2018; Yamada et al., 2013; Lammel et al., 2012). On the other hand, the ascending nociceptive pathways

also interact with these networks. For example, the spino-para-brachial circuits originate from the spinal dorsal horn and terminate in the lateral and external medial parabrachial nucleus (PBN) (Feil and Herbert, 1995). Populations of neurons in these regions send out projections to the midbrain regions, such as the amygdala and hypothalamus, which could be particularly activated by noxious stimuli (Bernard et al., 1996). Additionally, the midbrain DA neurons are known to acutely respond to biologically salient peripheral stimuli (e.g., nociceptive) with short-latency phasic bursts (Coizet et al., 2006; Maeda and Mogenson, 1982). Nonetheless, little is known about the circuits and mechanisms linking the ascending nociceptive pathways and the DA system in the midbrain and even less about potential mechanisms of altered VTA DA neuron activity in chronic-pain-induced depression.

In this study, we used pharmacology, electrophysiology, neuron projection tracing, immunofluorescence, optogenetics, and chemogenetics to elucidate midbrain circuits linking chronic pain and depression and to systematically investigate the role of the VTA DA neurons in the comorbid depression behavior in a trigeminal neuralgia model of chronic pain. We report a neural network linking the spinal trigeminal subnuelcus caudalis (SP5C) to the lateral PBM (LPBN) and the VTA DA neurons. We further show that this network is necessary for the development of depression-like symptoms associated with neuropathic pain development and that this network can be targeted to dissociate chronic pain and comorbid depression.

RESULTS

Chronic trigeminal neuralgia leads to depression-like behavior and increased activity of the VTA DA neurons

To investigate the mechanisms for the comorbid depression behavior in a chronic pain condition, we first established a trigeminal neuralgia mouse model of partial infraorbital nerve transection (pIONT) (Figures 1A and 1B). The neuropathic pain development in this model can be quantified as a frequency of specific face-grooming behavior (Vos et al., 1994). This behavior increased dramatically from day 1 after the pIONT surgery and sustained throughout the experimental timeline of 28–31 days (Figure 1C), indicating the neuropathic pain is chronic and persistent in this model. In a sham control group of mice, which underwent similar surgery except no transection of the nerve was performed, no induced neuropathic pain behavior was observed (Figure 1C). The following behavioral tests were performed at weekly intervals (for 4 weeks in total) following pIONT: the tail suspension test (TST), the forced swimming test (FST), the open field test (OFT), the sucrose preference test (SPT), and the social interaction test (SIT) under a subthreshold stress stimulation. The body weight was also measured (Figures S1A–S1G). In the TST and the FST that are often used in depression-like behavior studies, an increased immobility time (indicative of the depression-like behavior; Hao et al., 2019; Golden et al., 2011) was observed at the 4th week (28th day) in the pIONT mice in comparison with the sham group (Figure 1D; Figures S1A and S1B). Importantly, the locomotion abilities of the pIONT mice reflected by the traveling distance in the OFT remained unaffected (Figure S1C), indicating that the surgery and associated

pain did not affect locomotor activity as such. Hence, the increased immobility time in the TST and FST is unlikely to reflect a motor deficit associated with the surgery but instead is caused by a depression-like phenotype. A transient increase in the ratio of the time the mice spent at the central versus the peripheral area in the OFT test was observed at 7 days after the surgery, indicating a less anxious state of these mice; however, this result was not observed at later time points (Figure S1D). It should be noted that in the SPT, which is also often used as a test for depression-like behavior (Liu et al., 2018), no difference was observed between the pIONT and the sham mice (Figure S1E). This finding is not entirely unexpected because not all depression-like behaviors are present in different animal models (Hao et al., 2019). For SIT, we found a normal interaction ratio in both the pIONT and sham mice (Figure S1F). No differences in body weight between the pIONT and the sham mice were observed (Figure S1G).

Accumulating evidence (Krishnan et al., 2007; Chaudhury et al., 2013), including our own results (Li et al., 2017), suggest that the DA neurons in the VTA play important roles in depression-like behavior. Specifically, depression-like behavior is often associated with an increased burst firing of DA neurons in the VTA (Krishnan et al., 2007; Chaudhury et al., 2013; Li et al., 2017). To assess whether the depression-like behavior associated with pIONT neuropathic pain was also related to an increased VTA DA activity, we first recorded the VTA DA neuron firing *in vivo* and *in vitro* at the 28th–31st day after the pIONT surgery (Figure 1A), which are at time points at which pIONT mice already developed signs of depression-like behaviors. First, single-unit recordings were performed from VTA DA neurons of anesthetized mice; both the tonic and burst firing in these neurons (Figure 1E) were increased in the pIONT mice, in comparison with the sham mice (Figure 1F). DA neurons were identified by spike waveform (see STAR Methods). It should be noted that no such increase was seen at 14 days after the surgery (Figure S1H), when the depression-like behavior had not developed yet (Figures S1A and S1B). These findings indicate that the depression-like behavior correlated temporally with the increased firing of the VTA DA neurons. We also performed *in vitro* cell-attached patch clamp recordings on the VTA brain slices, and similarly, the firing of the VTA DA neurons was also increased in the pIONT mice, as compared to sham animals (28 days post-surgery); specifically, neurons in the lateral rather than the medial VTA area displayed such an increased activity (Huang et al., 2019; Figure 1G).

To summarize, these results suggest that the development of the depression-like behavior after pIONT is temporally correlated with increased firing of the VTA DA neurons.

Inhibition of increased firing of the VTA DA neurons reverses the depression-like behavior in the pIONT mice

To establish a direct link between the increased firing of the VTA DA neurons and the depression-like behavior seen in the pIONT mice, we tested if reducing the firing activity of the VTA DA neurons would reverse the depression-like behavior. To this end, retigabine (RTG), an opener of Kv7/KCNQ channels, was first used to inhibit the VTA DA neurons. Antiexcitatory Kv7 channels are expressed in VTA DA neurons, and RTG was shown to inhibit
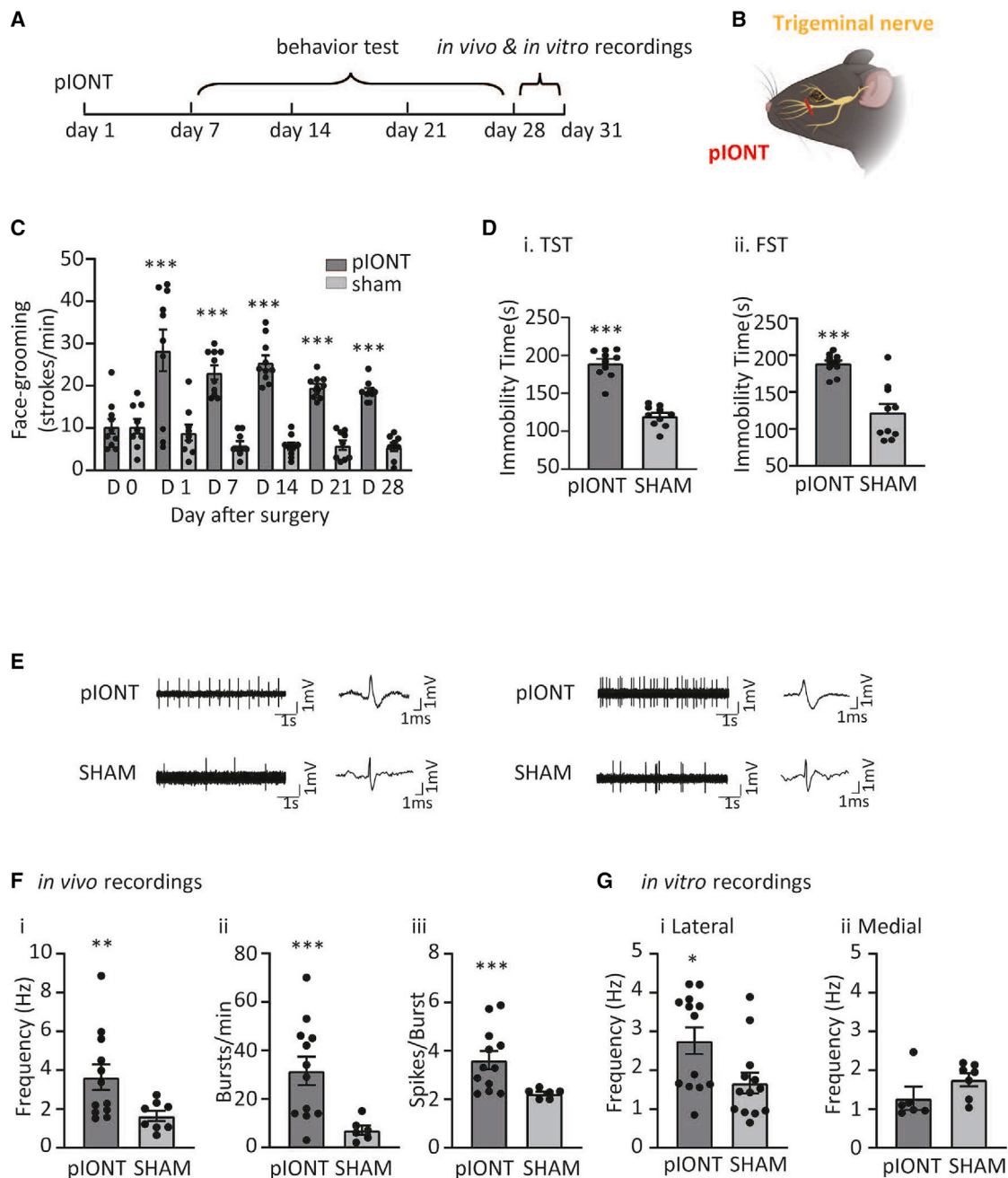
Figure 1. Chronic trigeminal neuralgia induces the depression-like behavior and increases the firing activity of the VTA DA neurons

(A) Schedule for the pIONT (partial infraorbital nerve transection) procedure and subsequent experiments.

(B) Schematic of the trigeminal nerve anatomy, showing infraorbital branch and the pIONT ligation/transection point (red line).

(C) Summary for trigeminal neuralgia, quantified as the frequency of face-grooming behaviors after the pIONT (n = 10) or sham (n = 9) surgeries, respectively; ***$p < 0.001$ (two-way repeated-measures ANOVA; Bonferroni post hoc test).

(D) Summary of the immobility times in tail suspension test (TST; i), and the forced swimming test (FST; ii) at the 28th day after the pIONT operation (n = 10; ***$p < 0.001$; two-tailed t test).

(E) Example traces of *in vivo* single-unit recordings of tonic (left) and burst firing (right) recorded from the VTA DA neurons of the pIONT and the sham-operated mice.

(F) Summarized firing frequency (i), number of bursts per minute (ii), and average number of spikes in a burst (iii); n = 13–15, **$p < 0.01$, ***$p < 0.001$, two-tailed t test.

(G) Firing frequency of the VTA DA neurons recorded *in vitro* from the brain slices of the lateral (i) and the medial (ii) VTA; n = 5–7, *$p < 0.05$, two-tailed t test. See also Figure S1.

Figure 2. RTG reduces the firing activity of the VTA DA neurons and alleviates the depression-like behaviors

(A) Schedule of the experimental procedures (left) and schematic illustration for drug delivery.

(B) Example recordings from the VTA DA neurons before and during the application of vehicle (ACSF, 0.4 μl) or RTG (200 μM, 0.4 μl), applied in sequence to the same neuron. The recordings were made using *in vivo* single-unit recordings 28 days after the pIONT or sham operations.

(C) Histogram showing the time course of RTG-induced inhibition on the VTA DA neuron firing frequency.

(D) Summary data for experiments as those shown in (B). The frequencies were quantified at 5 min after the ACSF or RTG application (n = 8, ***p < 0.001, one-way repeated-measures ANOVA with Bonferroni post hoc test).

(legend continued on next page)

these neurons (Li et al., 2017). We implanted into VTA a multi-channel pipette, which was used to record the single-unit firing of VTA DA neurons, as well as for local RTG (or vehicle) delivery (Figure 2A). Application of vehicle control (artificial cerebrospinal fluid [ACSF]) did not affect the firing of the VTA DA neuron; RTG (200 μM, 400 nL) on the other hand significantly and reversibly reduced the firing activity of the VTA DA neurons (Figures 2B–2D). A transient decrease in the firing frequency caused by the pressure from the drug-delivering pipette could be seen immediately following the drug application in some recordings (e.g., in Figure 2C); this artifact quickly recovered, followed by a persistent prominent inhibition of the firing by RTG (Figure 2C). Importantly, not only the total firing frequency but also the burst firing of the VTA DA neurons was reduced in the pIONT mice. Not surprisingly, the firing of the VTA DA neurons in the sham mice was also reduced by RTG (Figure 2E). We next applied RTG through a cannula implanted in the VTA and evaluated the depression-like behavior in the pIONT mice. The immobility time in the TST was first measured in both the sham and the pIONT mice at 28–31 days after surgery; at 24 h after the first test, RTG (200 μM, 400 nL) or ACSF was applied, and 15 min later, the TST was repeated. As expected, pIONT mice developed the depression-like behavior, manifested by increased immobility time in the TST; however, it was reversed by RTG (Figure 2Fi). Of note, RTG did not significantly affect the immobility time of the TST in the sham mice (Figure 2Fii).

Another important observation was that VTA-delivered RTG did not affect the pIONT-induced neuropathic pain behavior. Indeed, the face grooming intensity was not affected by local application of RTG into the VTA (Figure S2A). Furthermore, we also tested the effect of RTG on nocifensive behaviors that originated not from the trigeminal nerve but from the spinal nerve; in this regard, VTA-applied RTG did not affect the sensitivity of naive mice to noxious mechanical and thermal stimulation applied to the hind paws (Figures S2B and S2C). Thus, the data suggest that dampening the firing activity of the VTA DA neurons reduces chronic-pain-associated depressive behavior but not the pain itself. Here and in other similar experiments, we did not perform FST, as cannulated animals struggled to keep their heads above the water.

Specific manipulation of VTA DA firing activity affects the depression-like behavior of the pIONT neuropathic pain mice

The above results from the pharmacological tool (RTG), although strongly indicative, did not rule out the possibility that RTG could affect the depression-like behavior indirectly through targets outside the VTA DA neurons. To exclude this possibility, a more specific targeted modulation of the VTA DA neurons was needed. To this end, a chemogenetics strategy was used first. AAV-DIO-hM4D-mCherry (AAV, adeno-associated virus; DIO, cre-on) viral particles were injected into the

VTA of a dopamine transporter (DAT; specific marker of DA neurons)-Cre mouse line, and the firing of the VTA DA neurons was selectively inhibited by activation of hM4D receptor, expressed specifically in the DA neurons, by an artificial ligand, clozapine N-oxide (CNO). In this series of experiments, the pIONT surgery was performed on these DAT-Cre mice that were VTA injected with either the AAV-DIO-hM4D-mCherry or AAV-DIO-mCherry (control) viral particles at the 21st day post-surgery (Figure 3A). Immunofluorescence results confirmed the specific expression of the viral cargo in the VTA DA neurons (Figure 3B). One week later (28 days post-surgery), the TST was performed on these mice before and 15 min after the intraperitoneal (i.p.) injection of CNO (3.3 mg kg^{-1}) or vehicle (saline). At 24 h, later the FST was carried out on the same animals under same conditions as the TST. As shown in Figure 3C, CNO (but not vehicle) significantly reduced the immobility time in both the TST and the FST in the AAV-DIO-hM4D-mCherry-injected mice but not in the control-virus-injected mice (Figure 3D). Importantly CNO did not affect the immobility time in the TST and FST in the sham-operated mice which expressed hM4D in the VTA DA neurons (Figure S3A), and similar to RTG, CNO did not affect the pIONT-induced pain behavior (face grooming) (Figure S3B). These data again indicate that selective inhibition of VTA DA neurons reduced pain-associated depression but not the pain itself.
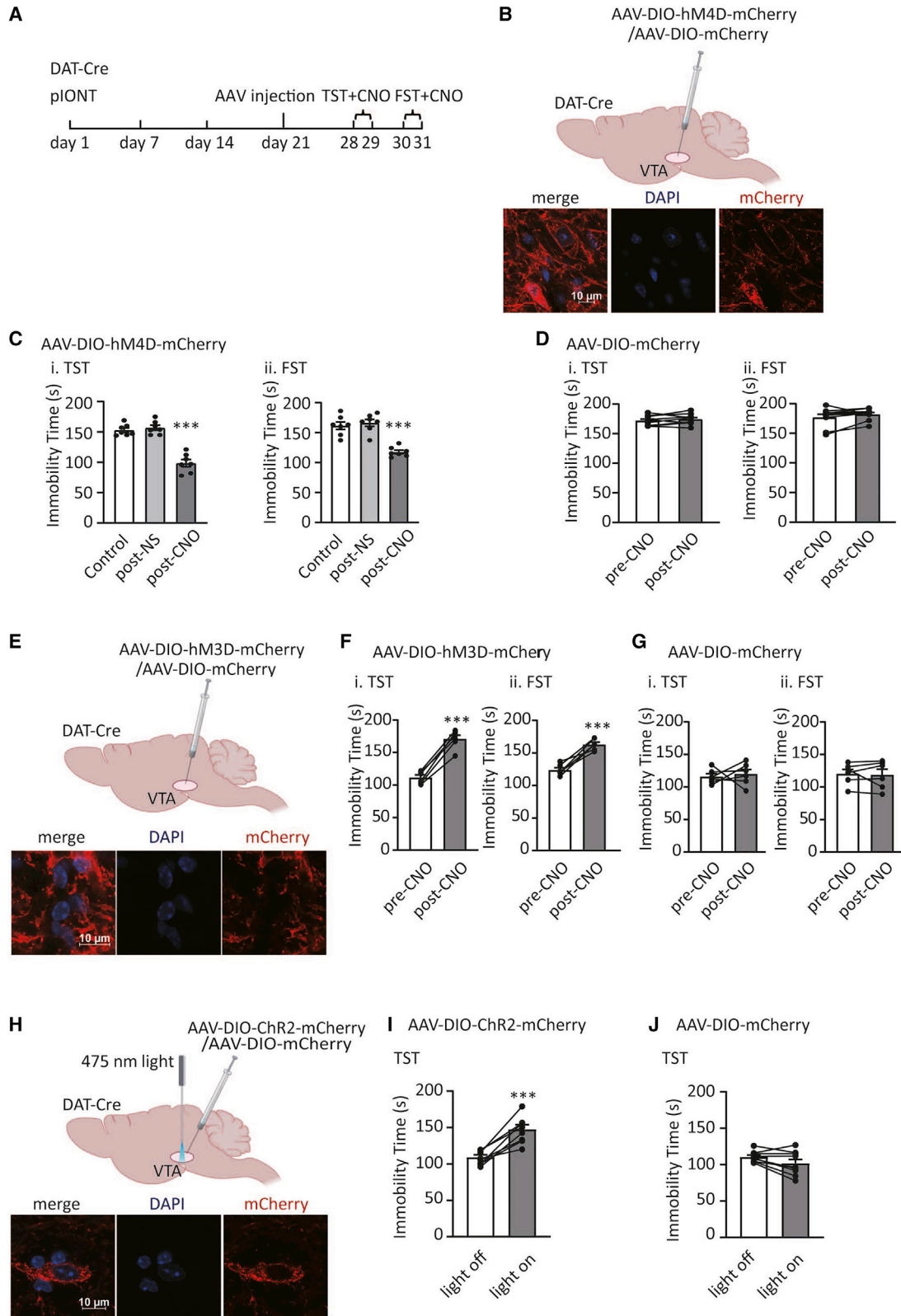
Next, we tested if activation of the VTA DA neurons in naive mice would induce the depression-like behavior. Viral particles carrying the gene for the excitatory DREADD receptor hM3D (AAV-DIO-hM3D-mCherry; Figure 3E) were delivered to the VTA of the naive mice, and tests were carried out before and after the application of CNO. In contrast to the inhibitory hM4D, expression of the hM3D would enable CNO to excite the VTA DA neurons. The immobility time in both the TST and FST was elevated after CNO administration in the AAV-DIO-hM3D-mCherry-injected mice (Figure 3F) but not in the AAV-DIO-mCherry (control)-injected mice (Figure 3G). Similar to inhibitory hM4D, activation of hM3D also did not affect the pain behavior of the pIONT mice (Figure S3C).

Additionally, an optogenetic strategy was also used to activate VTA DA neurons. In this case, AAV-DIO-ChR2-mCherry viral particles were delivered to the VTA of the DAT-Cre mouse line (Figure 3H). Activation of the ChR2 in the VTA DA neurons with the 475-nm laser illumination (by the VTA-implanted optical guide) also increased the immobility time in the TST (Figure 3I); this effect was not seen in the mice that received the control virus (AAV-DIO-mCherry; Figure 3J). The above chemogenic and optogenetic results lend further support to our hypothesis that the depression-like behavior developing in the pIONT mice is directly caused by an increased firing activity of the VTA DA neurons.

It should be noted however that optical stimulation of DA neurons may be acutely rewarding, and this could complicate the interpretation of the behavioral outcome of the TST test. This

(E) Summary data for the effects of RTG on the firing frequency (i), burst/min (ii), and spike/burst (iii) under in the pIONT-operated and the sham-operated mice (n = 5–10, *p < 0.05, paired t test).

(F) Summary data for the effects RTG and ACSF on the immobility time in the TST at 28 days after the pIONT or the sham operations. RTG (200 μM, 0.4 μl) was given through the cannula implanted into the VTA (n = 8, **p < 0.01, one-way repeated-measures ANOVA with Bonferroni post hoc test). The TST was performed before and 15 min after the infusion of either RTG or ACSF, with an interval of 24 h. See also Figure S2.

A

DAT-Cre
pIONT

			AAV injection	TST+CNO	FST+CNO

day 1   day 7   day 14   day 21   28 29   30 31

B

AAV-DIO-hM4D-mCherry
/AAV-DIO-mCherry

DAT-Cre

VTA

merge   DAPI   mCherry
10 μm

C AAV-DIO-hM4D-mCherry

i. TST

ii. FST

D AAV-DIO-mCherry

i. TST

ii. FST

E

AAV-DIO-hM3D-mCherry
/AAV-DIO-mCherry

DAT-Cre

VTA

merge   DAPI   mCherry
10 μm

F AAV-DIO-hM3D-mCherry

i. TST

ii. FST

G AAV-DIO-mCherry

i. TST

ii. FST

H

475 nm light

AAV-DIO-ChR2-mCherry
/AAV-DIO-mCherry

DAT-Cre

VTA

merge   DAPI   mCherry
10 μm

I AAV-DIO-ChR2-mCherry

TST

J AAV-DIO-mCherry

TST

(legend on next page)

issue should possibility be tested in a more directed experimental design in a future study.

Neuronal circuit linking VTA with LPBN

Because neuropathic pain is associated with the depressive phenotype, a link between the neural pathways of neuropathic pain and the VTA DA neurons, which control the emotions/mood, must exist. Thus, next we aimed to establish the neuronal circuits linking these two neurological phenomena. First, we used the c-Fos expression as an indicator of neurons, activated by the pIONT surgery. Immunofluorescence staining of c-Fos was performed in whole-brain slices from the pIONT mice and the sham control mice at the 28th day after the surgery. Increased c-Fos immunoreactivity was seen in the medial habenula, the laterodorsal tegmental nucleus, the ventromedial hypothalamic nucleus, the dorsomedial hypothalamic nucleus, the spinal trigeminal tract, median raphe nucleus, the locus coeruleus, and not surprisingly the VTA. Noteworthy, the spinal trigeminal nucleus caudalis (Sp5C), which is the nucleus receiving afferent input from the trigeminal ganglion (TG) (Edvinsson et al., 2020), and the LPBN that has been shown to be involved in the chronic pain conduction pathway were also labeled (Figure S4; Sun et al., 2020). A detailed c-Fos expression profile of pIONT and sham animals is listed in Table S1 (supplemental information). It should be noted that neural pathways that counteract the chronic pain could also contribute to the observed c-Fos activation.

To confirm a direct link between the VTA and the potential upstream sites activated by the pIONT injury, we traced the neurons projecting to the VTA by using retrograde labeling with retrobeads and, later, with Cre-dependent viral labeling (AAV-DIO-GFP) (Figures 4A–4C). Whole-brain images were first taken to track regions, which had been labeled by the VTA-injected retrobeads; multiple regions were found to have projections to the VTA (Figure 4B). For the theme of this study, we next focused on the LPBN, which (1) was identified as one of the regions sending the projections to the VTA (Figure 4B); (2) was activated by the pIONT surgery (Figure S4); and (3) has been reported to be involved in the development of neuropathic pain (Huang et al., 2019), including trigeminal neuralgia (Rodriguez et al., 2017). We then used a Vglut2-Cre mouse line, in which Cre is expressed

under control of a glutamatergic neuron marker, Vglut2 (Todd et al., 2003). These mice were VTA injected with the viral particles carrying Cre-dependent GFP (AAV-DIO-GFP); retrobeads were also injected simultaneously. We then evaluated the appearance of retrogradely labeled neuron somata in the LPBN. As shown in Figure 4C, neurons labeled with both GFP and retrobeads were clearly visible in the LPBN (Figure 4C, arrowheads). Of note, most of the neurons positively labeled with retrobeads (labeling all LPBN-to-VTA projecting neurons) were also labeled with GFP (labeling glutamatergic LPBN-to-VTA projecting neurons), indicating that most of the LPBN neurons projecting to the VTA were glutamatergic neurons.
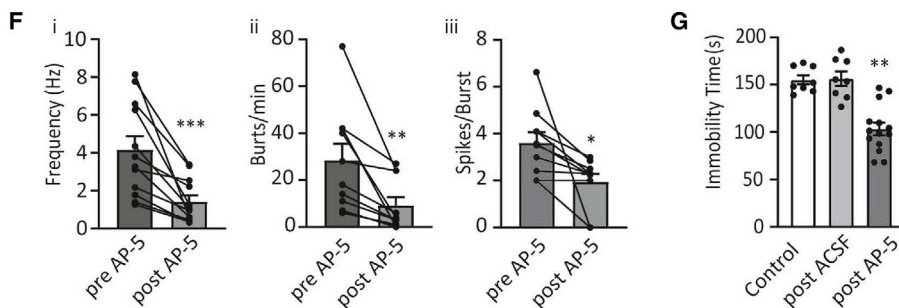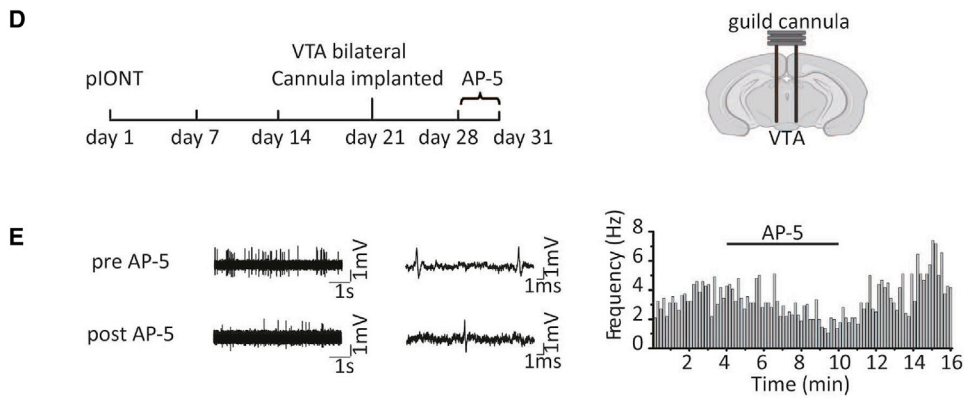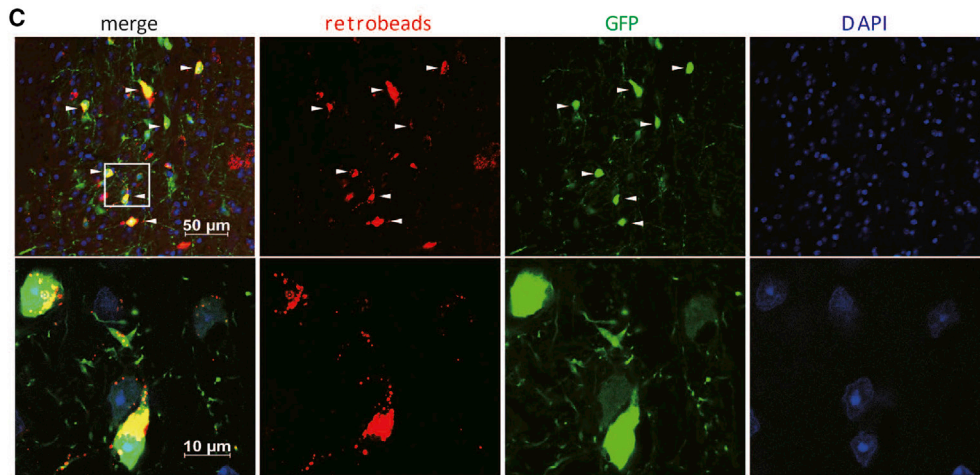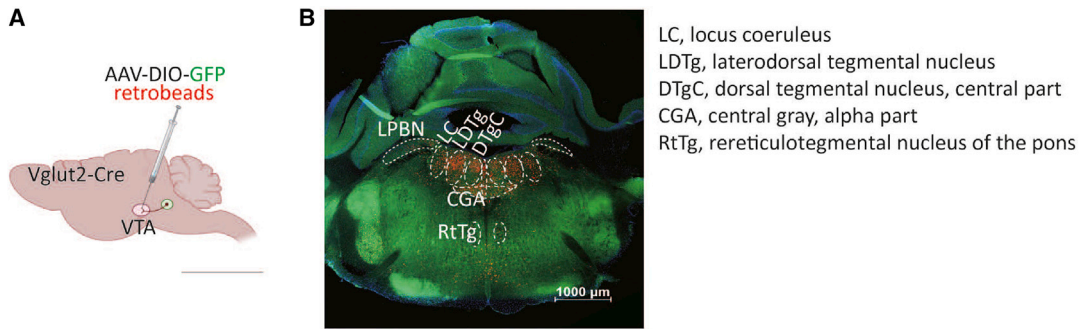
LPBN-VTA projections regulate the depressive-like behavior

To test if the above-identified LPBN-VTA glutamatergic projections are involved in regulation of the depression-like behavior, we first used local VTA application of glutamatergic antagonist AP-5 to block the glutamatergic input to the VTA, and the effect of this maneuver on the depression-like behavior was observed. AP-5 (200 μM, 400 nL) applied locally to the VTA of the pIONT mice 28 days after the surgery through the multi-channel pipette (Figure 4D) reversibly reduced the firing activity of the VTA DA neurons (Figure 4E), including the total firing frequency and the burst activity (Figure 4F). At the same concentration and volume, AP-5 (but not the vehicle, ACSF) reduced the immobility time in the TST (Figure 4G). On the other hand, AP-5 did not affect the immobility time in the sham-operated mice (Figure S5Ai). Similar to RTG chemogenic and optogenetic inhibition of VTA DA neurons, AP-5 also did not affect the pain behavior (face-grooming time) in the pIONT mice 28–31 days after the surgery (Figure S5Aii). These experiments suggest that blocking excitatory glutamatergic input to VTA selectively inhibits depressive-like behavior associated with chronic pain but not the pain itself.

In the above experiments, AP-5 abolished all types of glutamatergic transmission, including the input from distant projections or from local VTA circuits. To specifically test the function of glutamatergic projections from LPBN to the VTA DA neurons, the glutamatergic LPBN-VTA pathway was specifically inhibited using the inhibitory opsin NpHR. In these experiments, the pIONT surgery was performed on the Vglut2-Cre mice, and the viral

---

Figure 3. Specific manipulations with the VTA DA neuron activity alter depression-like behaviors

(A) Specific inhibition of the VTA DA neuron activity was realized with the use of chemogenetic activation of the hM4D receptor selectively expressed in the VTA DA neurons through the DAT-controlled Cre activity; schematic depicts the schedule of experimental procedures.

(B) Top, schematic illustrating the injection of the viral construct carrying the hM4D receptor (AAV-DIO-hM4D-mCherry) or the control virus (AAV-DIO-mCherry) into the VTA of the DAT-Cre mice (21 days after the pIONT operation). Bottom, mCherry fluorescence was clearly visible in the VTA DA neurons; nuclear DAPI (4′,6-diamidino-2-phenylindole) labeling is in blue.

(C and D) Specific inhibition of the VTA DA neurons in the pIONT mice reduced depression-like behaviors. The immobility time of the AAV-DIO-hM4D-mCherry-injected (C) and the AAV-DIO-mCherry-injected (D) mice in the TST (i) or the FST (ii) were measured before and 15 min after the administration of CNO (0.33 mg/kg, i.p.); there was a 24-hr interval between the tests (n = 7, **p < 0.01, ***p < 0.001, one-way repeated-measures ANOVA with Bonferroni post hoc test [C] or paired t test [D]).

(E) Specific activation of the VTA DA neurons was achieved with the use of the hM3D receptor selectively expressed in the VTA DA neurons through DAT-controlled Cre activity (DAT-Cre mice); specific expression of hM3D in the VTA DAT neurons was confirmed by the co-expressed mCherry (bottom panel).

(F and G) The mice injected with the hM3D-carrying virus (F) and with the control virus (G) were subjected to TST (i) or FST (ii), and the immobility time was quantified (n = 6, ***p < 0.001, paired t test).

(H) Optogenetic activation of the VTA DA neurons in the naive mice. AAV-DIO-ChR2-mCherry or AAV-DIO-mCherry (control) viral particles were injected into the VTA of DAT-Cre mice. The ChR2 was activated by a 475-nm laser through an implanted optical fiber.

(I and J) The immobility time in the TST of mice with (I) and without (J) ChR2 expression were measured under 475-nm (20 Hz, 5 pulses per 10 s) light off and light on; n = 8, ***p < 0.001, paired t test. See also Figure S3.

A

AAV-DIO-GFP
retrobeads

Vglut2-Cre

VTA

B

LPBN LDTg DTgC

CGA

RtTg

1000 μm

LC, locus coeruleus
LDTg, laterodorsal tegmental nucleus
DTgC, dorsal tegmental nucleus, central part
CGA, central gray, alpha part
RtTg, rereticulotegmental nucleus of the pons

C

merge	retrobeads	GFP	DAPI

50 μm

10 μm

D

pIONT

VTA bilateral
Cannula implanted   AP-5

day 1   day 7   day 14   day 21   day 28   day 31

guild cannula

VTA

E

pre AP-5   1mV   1s   1mV   1ms
post AP-5   1mV   1s   1mV   1ms

AP-5

Frequency (Hz)

Time (min)

F

i
Frequency (Hz)
pre AP-5   post AP-5   ***

ii
Burts/min
pre AP-5   post AP-5   **

iii
Spikes/Burst
pre AP-5   post AP-5   *

G
Immobility Time(s)
Control   post ACSF   post AP-5   **

(legend on next page)

particles carrying Cre-dependent NpHR (AAV-DIO-NpHR-eYFP; NpHR, Halorhodopsin; eYFP, a mutation of yellow fluorescent protein) were injected into the LPBN. The LPBN-VTA glutamatergic projections were then specifically inhibited by activation of the NpHR at the nerve terminals in the VTA through the 590-nm laser illumination delivered through the implanted light guide (Figures 5A and 5B). The viral construct was well expressed in the LPBN glutamatergic neuron somata and at the projection terminals around the VTA DA neurons (Figure 5C). The immobility time in the TST was significantly reduced in pIONT mice upon optogenetic stimulation (Figure 5D), suggesting that inhibition of the LPBN-to-VTA glutamatergic projections was able to reverse the depressive-like behavior of the pIONT mice. However, in a similar setting, activation of NpHR did not affect the immobility time in the TST performed on sham mice (Figure S5B and S5C).

A similar strategy was also applied on the naive mice, except that the inhibitory NpHR was replaced with the excitatory ChR2 (AAV-DIO-ChR2-mCherry). In this case, the LPBN-to-VTA glutamatergic input was activated to test if it would confer the naive mice with the depression-like behavior (Figures 5E–5H). Indeed, illumination of the VTA with the 475-nm laser significantly increased the immobility time in mice injected with the ChR2-carring virions (Figure 5Hi) but not control virions (Figure 5Hii).

A direct Sp5C-LPBN-VTA circuit controls the depression-like behavior in the mice with chronic trigeminal neuralgia

In our c-Fos experiments (Figure S4; Table S1), the increased c-Fos fluorescence was also evident in the Sp5C, which is a nucleus relaying the pain signals from the TG to the higher brain centers (Hargreaves, 2011; Pradier et al., 2019). We reasoned that there could be a circuit connecting the Sp5C with the VTA, which can possibly involve projections through the LPBN because the link between the Sp5C and the LPBN has been reported (Edvinsson et al., 2020). To establish if such a connection exists, we first used the retrobeads and the AAV-DIO-GFP injected into the LPBN of Vglut2-Cre mice. Two weeks after the injection, the retrobeads and GFP signals were indeed clearly visible in the Sp5C (Figures 6A and 6B). To test if there are direct monosynaptic projections from the Sp5C to the LPBN and from the LPBN to the VTA, we used the *trans*-monosynaptic retrograde labeling approach. To this end, two viral constructs carrying AAV-DIO-TVA-tdTomato and AAV-DIO-RVG were injected into the LPBN of Vglut2-Cre mice as helpers to specifically express these rabies virus (RV) components in the glutamatergic cells projecting from the LPBN to the VTA and to enable future RV infection and *trans*-monosynaptic tracing (Suzuki et al., 2020) to the Sp5C. Four weeks later, the replication-deficient RV (RV-ENVA-ΔG-eGFP) was injected into the VTA (Figure 6C). This maneuver enables simultaneous tracing of direct projections from the LPBN to the VTA and monosynaptic projections from the Sp5C to the LPBN. After one more week, the GFP was identified at the Sp5C (Figure 6D), whereas tdTomato was detected in VTA. These results confirmed the existence of a direct Sp5C-to-LPBN-to-VTA circuit.

Next, we tested if this Sp5C-LPBN-VTA circuit was involved in the depression-like behavior of the pIONT neuropathic pain mice. The pIONT surgery was performed on the Vglut2-Cre mice, and the AAV-DIO-NpHR-eYFP was injected to the Sp5C, which enabled the glutamatergic-neuron-specific expression of NpHR in the projections from the Sp5C to the LPBN (Figure 6E). After one week, the NpHR-eYFP was clearly detectable in the terminals of glutamatergic Sp5C projections in the LPBN. These terminals were inhibited by a laser light delivered through the optical fiber implanted into the LPBN (Figures 6F and 6G). In AAV-DIO-NpHR-eYFP-injected mice, light stimulation significantly reduced immobility time in the TST (Figure 6Hi), an effect that was not seen in mice injected with AAV-DIO-eYFP (control; Figure 6Hii). These experiments confirmed that the Sp5C-LPBN-VTA circuit is a functional pathway producing depressive behavior in chronic pain states.

DISCUSSION

In this study, we present cellular, anatomical, and functional evidence for the existence of a neuronal circuit linking the Sp5C, LPBN, and VTA. We show that this pathway mediates the development of depressive behavior comorbid to chronic cranial neuropathic pain. The major findings of this study include the following: (1) glutamatergic projections from the Sp5C innervate the glutamatergic neurons in the LPBN, which project to the VTA and modulate the activity of the DA neurons in this nucleus. (2) This Sp5C-LPBN-VTA circuit is activated under a state of chronic neuropathic pain, which ultimately results in an increased firing activity of the VTA DA neurons. (3) Overactivity of the VTA DA

Figure 4. Glutamatergic projections from LPBN to VTA control depression-like behaviors
(A) Retrobeads (100 nL) and Cre-dependent virus AAV-DIO-GFP were injected to the VTA of Vglut2-Cre mice to visualize a Vglut2-controlled expression of GFP and retrograde tracing in the LPBN.
(B) Retrobead fluorescence in an image from a 30-μμ coronal brain section from the ventral side at Bregma −5.34 mm. The brain regions most prominently labeled by the retrobeads are shown with dotted ellipses.
(C) Higher-magnification images showing the retrobeads and GFP fluorescence in the LPBN neuron. Co-labeling of GFP and retrobeads is indicated in the top panel (arrowheads). The area indicated by the white square is shown in the bottom panel with higher magnification.
(D) Experimental schedule (left) and schematic of a cannula placement (right) for the local application of the NMDA blocker AP-5. The cannula was implanted into the VTA at 21 days after the pIONT/sham operation.
(E) Example traces of single-unit recordings showing firing of the VTA DA neurons before and during AP-5 (200 μM, 300 nL) application (left). Shown on the right is the time course for the effect of AP-5 on the firing frequency.
(F) Summary data for effects of AP-5 on firing frequency (i), burst number/min (ii), and spike number/burst (iii); n = 10–12, ***p < 0.001, **p < 0.01, *p < 0.05, paired t test.
(G) Summary data for effects of AP-5 and the vehicle (ACSF) on the immobility time in the TST. The TST was performed 15 min after application, with an interval of 24 h between ACSF and AP-5; n = 14, ***p < 0.001, one-way repeated-measures ANOVA with Bonferroni post hoc test. See also Figures S4 and S5.
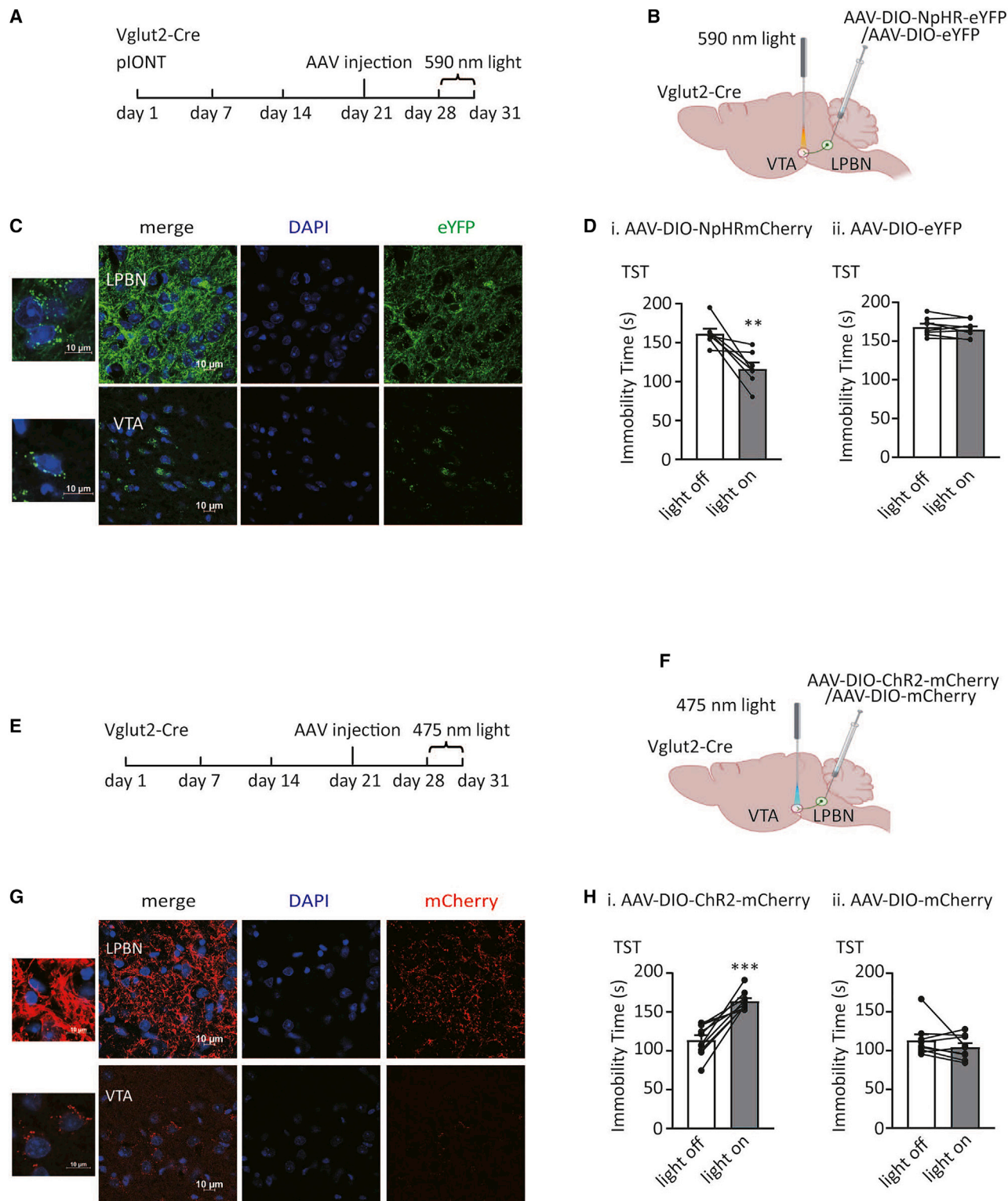
A

Vglut2-Cre
pIONT

| day 1 | day 7 | day 14 | day 21 | day 28 | day 31 |
AAV injection   590 nm light

B

590 nm light ———— AAV-DIO-NpHR-eYFP
/AAV-DIO-eYFP

Vglut2-Cre

VTA   LPBN

C

merge   DAPI   eYFP

LPBN

10 μm   10 μm

VTA

10 μm   10 μm

D   i. AAV-DIO-NpHRmCherry   ii. AAV-DIO-eYFP

TST   TST

(Immobility Time (s), light off / light on — ** in i.)

E

Vglut2-Cre

| day 1 | day 7 | day 14 | day 21 | day 28 | day 31 |
AAV injection   475 nm light

F

475 nm light ———— AAV-DIO-ChR2-mCherry
/AAV-DIO-mCherry

Vglut2-Cre

VTA   LPBN

G

merge   DAPI   mCherry

LPBN

10 μm   10 μm

VTA

10 μm   10 μm

H   i. AAV-DIO-ChR2-mCherry   ii. AAV-DIO-mCherry

TST   TST

(Immobility Time (s), light off / light on — *** in i.)

Figure 5. Selective manipulations with the glutamatergic LPBN-VTA projections alter the depression-like behaviors

(A) Experimental schedule.

(B) Schematic of viral labeling. AAV-DIO-NpHR-eYFP/AAV-DIO-eYFP (200 nL) virions were injected into the LPBN of the Vglut2-Cre mice bilaterally at 21 days after the pIONT operation, and an optical fiber was implanted in the VTA. The 590-nm laser was used to activate NpHR.

(legend continued on next page)

neurons underlies the depression behavior developed under a state of chronic neuropathic pain. (4) Pharmacological or genetic interventions inhibiting the firing of the VTA DA neurons reverse the depressive behaviors, thus "uncoupling" chronic pain from comorbid depression. With a high proportion of depression symptoms seen in patients with chronic pain (Cheng et al., 2017; Tang et al., 2016) and a reciprocal interaction between depression and chronic pain (Bair et al., 2003; IsHak et al., 2018), our findings provide a framework for the underlying networks and mechanisms linking these two neurological phenomena. These findings may also aid the diagnosis and treatment of these debilitating conditions, which often present a challenge in clinical practice (Bair et al., 2003; IsHak et al., 2018).

Although it has long been hypothesized that neural processing of chronic pain and its affective aspects, including those leading to depression, could share common neural pathways and mechanisms, they have not been clearly established. Here, we are filling a part of this void by establishing a VTA-DA-neuron-centered pathway, which orchestrates the depression behavior in a chronic pain condition. Recent evidence suggests that the altered firing activity, especially the burst firing of the VTA DA neurons, which encodes the release of dopamine (Gonon, 1988; Grace, 1991), directly governs the depression behavior (Krishnan et al., 2007; Chaudhury et al., 2013; Tye et al., 2013) and regulates neuropathic pain (Huang et al., 2020). The activity of the VTA DA neurons is under complex control by both the intrinsic as well as the regulatory activity (Overton and Clark, 1997; Zweifel et al., 2009; Omelchenko et al., 2009; Dobi et al., 2010). In this study, we provide evidence that there is a direct pathway linking Sp5C with LPBN and LBPN with the VTA DA neuron system. The Sp5C, in turn, receives direct input from the trigeminal nucleus (Sessle, 2000), where nociceptive signals produced by peripheral nerve injury originate. Multiple pieces of evidence, including pharmacological, neuron projection tracing, and chemo- and optogenetic results, presented here strongly support this claim. Thus, the experiments using the RV to trace *trans*-monosynaptic connections suggest that the connection between the Sp5C and the LPBN and between the LPBN and the VTA must indeed be direct (Figure 6). Under the condition of persistent noxious input (as in the case of the pIONT neuropathic pain model), the Sp5C-LPBN-VTA pathway must be persistently activated, which was manifested by the increased c-Fos expression in the Sp5C, the LPBN, and the VTA (as well as in some other brain areas). The persistent activation of this pathway is likely to exert a plastic effect on the VTA DA neurons and the downstream targets of the VTA DA neuron projections, which ultimately establish a basis for the observed depression behavior. This notion is supported by the observation that the

depression behavior develops with a considerable delay (over 3 weeks) after the pIONT surgery, long after the onset of the painful behavior that normally is already evident the next day after the surgery. This delayed development of depression behavior was also reported in a different neuropathic model, namely, spared nerve injury (SNI) (Zhou et al., 2019).

A direct glutamatergic link from the Sp5C to the LPBN and to the VTA DA neurons has not been described before, although monosynaptic inputs to the VTA DA neurons from the LBPN were demonstrated (Watabe-Uchida et al., 2012; Ogawa et al., 2014; Beier et al., 2015), including a glutamatergic projection from the LPBN to the VTA that has just been reported to control pain behavior (Yang et al., 2021). Our current study ascribes the LBPN glutamatergic neurons projecting to the VTA DA neurons with a functional role in mediating chronic-pain-induced depression behavior. Recently, the glutamatergic neurons in the PBN were found to be responsible not only for relaying basal nociception but also for processing neuropathic pain in a model of common peroneal nerve (CPN) ligation (Sun et al., 2020). Our data further extend this line of evidence by adding a trigeminal neuralgia neuropathic pain model to the list; collectively, these findings suggest that the LPBN could be a common relay pathway for the neuropathic pain and depression comorbidity.

A different projection pathway was recently described for the depression associated with SNI-induced neuropathic pain (Zhou et al., 2019). This pathway involves the 5-hydroxytryptamine (5-HT) neurons in the DRN to somatostatin (SOM)-expressing and non-SOM interneurons in the central nucleus of the amygdala (CeA), which then project directly to the LHb, an area known for its involvement in depression (Yang et al., 2018). Yet, it is tempting to speculate that this pathway may ultimately detour to the VTA DA neurons because dense direct projections from both the DRN and the LHb to the VTA DA neurons have been described (Lammel et al., 2012; Watabe-Uchida et al., 2012; Ogawa et al., 2014). Thus, these midbrain monoamine circuits regulated by the inputs from the pain pathways emerge as central integration hubs for the processing of pain and the affective behaviors.
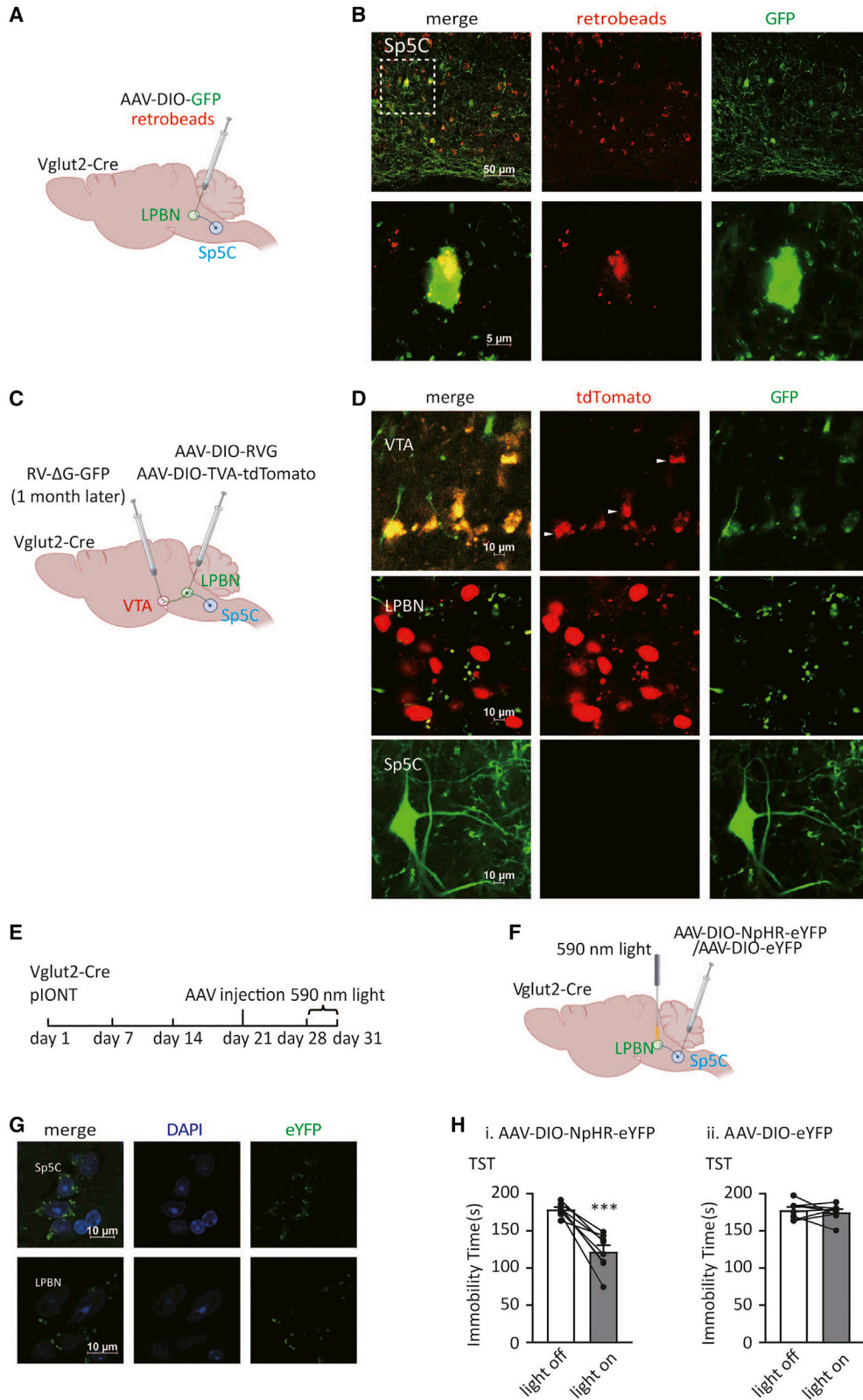
The LPBN is known for involvement in both somatic and craniofacial pain transmission (Sun et al., 2020; Hermanson and Blomqvist, 1996). Importantly, craniofacial stimuli appear to be stronger activators of the nociceptive LPBN (Hermanson and Blomqvist, 1997), and a stronger affective aspect of the craniofacial pain was described, as compared to pain arising from the spinal somatosensory stimuli (Schmidt et al., 2019). One reason for these differences could be the presence of a dual pathway from the TG, namely, the TG-LPBN pathway and the TG-Sp5C-LPBN pathway. In contrast, a single indirect pathway from the dorsal root ganglion (DRG), namely, the

(C) eYFP fluorescence confirmed the expression of NpHR at the projection terminals of the glutamatergic neurons from the LPBN (top panel) around the neuronal cell bodies in VTA (bottom panel).

(D) Summary data for effects of the 590-nm laser illumination (constant) on the immobility time in the TST. The TST was performed before and during the laser illumination on the mice at 28 days after the pIONT surgery; n = 8, **p < 0.001, paired t test.

(E–G) Selective activation of the glutamatergic neurons in the LPBN projecting to the VTA DA neurons increased the immobility time of the TST in the naive mice. AAV-DIO- ChR2-mCherry/AAV-DIO-mCherry (200 nL) virions were injected bilaterally to the LPBN of the naive Vglut2-Cre mice (E), and an optical fiber was implanted into the VTA. A 475-nm laser was used to activate ChR2 (F). (G) Expression of the ChR2 (visualized by mCherry) at the projection terminals of the glutamatergic neurons from the LPBN (top panel) and around the neuronal cell bodies in VTA (bottom panel).

(H) Activation of ChR2 with 475-nm illumination in the VTA increased the immobility in the TST in the ChR2-expressing (i) but not in the non-ChR2-expressing control (ii) mice; n = 10, ***p < 0.001, paired t test. See also Figures S5 and S6.

A

AAV-DIO-GFP
retrobeads

Vglut2-Cre

LPBN

Sp5C

B   merge   retrobeads   GFP

Sp5C

50 μm

5 μm

C

RV-ΔG-GFP
(1 month later)

AAV-DIO-RVG
AAV-DIO-TVA-tdTomato

Vglut2-Cre

VTA   LPBN

Sp5C

D   merge   tdTomato   GFP

VTA

10 μm

LPBN

10 μm

Sp5C

10 μm

E

Vglut2-Cre
pIONT

AAV injection   590 nm light

day 1   day 7   day 14   day 21 day 28 day 31

F

590 nm light

AAV-DIO-NpHR-eYFP
/AAV-DIO-eYFP

Vglut2-Cre

LPBN   Sp5C

G   merge   DAPI   eYFP

Sp5C

10 μm

LPBN

10 μm

H   i. AAV-DIO-NpHR-eYFP   ii. AAV-DIO-eYFP

TST   TST

***

(legend on next page)

DRG-spinal dorsal horn-LPBN (Rodriguez et al., 2017), was found for spinal somatosensory transmission. Future studies shall reveal whether this differential affective processing of spinal versus trigeminal pain involves distinct subpopulations of the LBPN neurons or is a stimulation-intensity-coded phenomenon.

Another important notion is that although the depression-like behavior in the pIONT mice was clearly caused by neuropathic pain from the trigeminal nerve injury, we have strong reasons to believe that depression and pain are controlled and processed separately in the brain. Thus, various pharmacological, chemogenetic, and optogenetic manipulations with VTA DA neuron activity, which reversed the depression-like behaviors, did not affect the neuropathic pain behaviors. This is further supported by the observation that the depression-like behavior developed with a significant delay after the pIONT procedure, long after the pain behavior was established. Thus, chronic pain and depression, although inter-related, clearly are distinct neurological phenomena; moreover, as we show in this study, pain and comorbid depression can be disassociated by manipulations with the Sp5C-LPBN-VTA pathway.

An important observation from this study was that the depression behavior developed in the pIONT neuropathic pain mice could be reversed by pharmacological intervention using a Kv7/KCNQ channel opener, RTG. When infused directly into the VTA, RTG reduced the firing activity of the VTA DA neurons, and, consistent with previous studies (Li et al., 2017; Friedman et al., 2016; Tan et al., 2020), led to the reversal of the depression behavior. This result potentially opens a window of opportunity for RTG or similar drugs to be used for the treatment of the depression symptoms comorbid to chronic pain. Importantly, RTG and other Kv7 openers have analgesic efficacy, most likely acting through the peripheral nervous system (Du et al., 2014; Hayashi et al., 2014). Thus, these drugs could be beneficial for the treatment of both depression and pain.

It should also be emphasized that the relationships between chronic pain and depression are complex; not only could chronic pain trigger depression but also depression is a major modulator of the chronic pain states (Simon et al., 1999). This mutual penetration is best reflected in the fact that some antidepressants are the first-line drugs for the treatment of neuropathic pains (Obata, 2017; Finnerup et al., 2010). We believe that the present study sheds light on the intricate relationships between chronic pain and depression by identifying a neural pathway feeding into depression circuits from the pain matrix; however, the full complexity of these relationships is yet to be discovered and should be investigated in future studies.

Limitations of the study

In this study, only male mice were used, mainly due to the use of the social defeat depression model that excludes the possibility of using female mice. The sex hormones could have a significant effect on the pain responses, the depression behaviors, and the underlying mechanisms. Thus, interpretation of the current results in a more general scope should be carefully considered.

STAR★METHODS

Detailed methods are provided in the online version of this paper and include the following:

- KEY RESOURCES TABLE
- RESOURCE AVAILABILITY
  - Lead contact
  - Materials availability
  - Data and code availability
- EXPERIMENTAL MODEL AND SUBJECT DETAILS
- METHOD DETAILS
  - Animal models of neuropathic pain
  - Cannula implantation and intracerebral drug infusion
  - Viral injections
  - Neuron projection tracing
  - Optogenetics
  - Chemogenetics
  - Electrophysiology
  - Immunohistochemistry
  - Behavioral assessment of neuropathic pain and depressive-like behavior
  - cFos immunofluorescence
- QUANTIFICATION AND STATISTICAL ANALYSIS

SUPPLEMENTAL INFORMATION

Supplemental information can be found online at https://doi.org/10.1016/j.celrep.2021.109936.

Figure 6. Direct glutamatergic projection pathway linking Sp5C, LPBN, and VTA governs the chronic-pain-induced depression behaviors

(A and B) Projections from the Sp5C to the LPBN identified through retrograde labeling. Retrobeads and AAV-DIO-GFP were injected in the LPBN of Vglut2-Cre mice (A). Co-staining with retrobeads and GFP is visible in multiple neurons in the Sp5C (B).

(C) Schematic for the *trans*-monosynaptic retrograde projection tracing of the Sp5C-LPBN-VTA pathway. Viruses used, the injection sites, and the time of injection are indicated. The Cre-dependent constructs were injected into the Vglut2-Cre mice, thus restricting the expression to the glutamatergic neurons.

(D) Visualization of the expression of tdTomato and GFP in the VTA, the LPBN, and the Sp5C. The tdTomato was prominently visible in the glutamatergic neuron somata in the LPBN (middle panel) and in presumed projection terminals (from LPBN) in the VTA (top panel, arrowheads); tdTomato was not detected in the Sp5C (bottom panel). This pattern indicates a restricted expression of the tdTomato in the glutamatergic neurons of the LPBN projecting to the VTA. GFP, injected into the VTA, was clearly expressed in the glutamatergic neuron somata in the Sp5C (bottom panel), indicating a monosynaptic connection between the glutamatergic neurons in the Sp5C and the LPBN that projected to the VTA.

(E) Schematic for testing the effects of Sp5C-LPBN pathway inhibition on the depression behaviors by using optogenetic manipulation.

(F) Schematic indicating viruses used and injection and illumination sites. The viruses (200 nL) were injected bilaterally to the Sp5C of the Vglut2-Cre mice at 21 days after the pIONT operation, and an optical fiber was implanted in the LPBN; a 590-nm laser light was used for NpHR stimulation.

(G) Following Sp5C injection, NpHR was expressed at the terminals of Sp5C-LPBN-projecting glutamatergic neurons in the LPBN (visualized by eYFP fluorescence).

(H) Summary data for the effects of inhibiting the glutamatergic projections from the Sp5C to the LPBN on the immobility time in the TST; illumination of the LPBN with a 590-nm laser reduced the immobility time in NpHR expression mice (i) but not in the control mice (ii); n = 8, ***p < 0.001, paired t test.

REFERENCES

Arnow, B.A., Hunkeler, E.M., Blasey, C.M., Lee, J., Constantino, M.J., Fireman, B., Kraemer, H.C., Dea, R., Robinson, R., and Hayward, C. (2006). Comorbid depression, chronic pain, and disability in primary care. Psychosom. Med. 68, 262–268.

Bair, M.J., Robinson, R.L., Katon, W., and Kroenke, K. (2003). Depression and pain comorbidity: a literature review. Arch. Intern. Med. 163, 2433–2445.

Beier, K.T., Steinberg, E.E., DeLoach, K.E., Xie, S., Miyamichi, K., Schwarz, L., Gao, X.J., Kremer, E.J., Malenka, R.C., and Luo, L. (2015). Circuit Architecture of VTA Dopamine Neurons Revealed by Systematic Input-Output Mapping. Cell 162, 622–634.

Bernard, J.F., Bester, H., and Besson, J.M. (1996). Involvement of the spino-parabrachio -amygdaloid and -hypothalamic pathways in the autonomic and affective emotional aspects of pain. Prog. Brain Res. 107, 243–255.

Berridge, K.C. (1990). Comparative Fine Structure of Action: Rules of Form and Sequence in the Grooming Patterns of Six Rodent Species. Behaviour 113, 21–56.

Blier, P., and Abbott, F.V. (2001). Putative mechanisms of action of antidepressant drugs in affective and anxiety disorders and pain. J. Psychiatry Neurosci. 26, 37–43.

Cao, J.L., Covington, H.E., III, Friedman, A.K., Wilkinson, M.B., Walsh, J.J., Cooper, D.C., Nestler, E.J., and Han, M.H. (2010). Mesolimbic dopamine neurons in the brain reward circuit mediate susceptibility to social defeat and antidepressant action. J. Neurosci. 30, 16453–16458.

Chaudhury, D., Walsh, J.J., Friedman, A.K., Juarez, B., Ku, S.M., Koo, J.W., Ferguson, D., Tsai, H.C., Pomeranz, L., Christoffel, D.J., et al. (2013). Rapid regulation of depression-related behaviours by control of midbrain dopamine neurons. Nature 493, 532–536.

Cheng, J., Long, J., Hui, X., Lei, D., and Zhang, H. (2017). Effects of microvascular decompression on depression and anxiety in trigeminal neuralgia: A prospective cohort study focused on risk factors and prognosis. Clin. Neurol. Neurosurg. 161, 59–64.

Cohen, J.Y., Haesler, S., Vong, L., Lowell, B.B., and Uchida, N. (2012). Neuron-type-specific signals for reward and punishment in the ventral tegmental area. Nature 482, 85–88.

Coizet, V., Dommett, E.J., Redgrave, P., and Overton, P.G. (2006). Nociceptive responses of midbrain dopaminergic neurones are modulated by the superior colliculus in the rat. Neuroscience 139, 1479–1493.

Dobi, A., Margolis, E.B., Wang, H.L., Harvey, B.K., and Morales, M. (2010). Glutamatergic and nonglutamatergic neurons of the ventral tegmental area establish local synaptic contacts with dopaminergic and nondopaminergic neurons. J. Neurosci. 30, 218–229.

Du, X., Hao, H., Gigout, S., Huang, D., Yang, Y., Li, L., Wang, C., Sundt, D., Jaffe, D.B., Zhang, H., and Gamper, N. (2014). Control of somatic membrane potential in nociceptive neurons and its implications for peripheral nociceptive transmission. Pain 155, 2306–2322.

Edvinsson, J.C.A., Viganò, A., Alekseeva, A., Alieva, E., Arruda, R., De Luca, C., D'Ettore, N., Frattale, I., Kurnukhina, M., Macerola, N., et al.; European Headache Federation School of Advanced Studies (EHF-SAS) (2020). The fifth cranial nerve in headaches. J. Headache Pain 21, 65.

Feil, K., and Herbert, H. (1995). Topographic organization of spinal and trigeminal somatosensory pathways to the rat parabrachial and Kölliker-Fuse nuclei. J. Comp. Neurol. 353, 506–528.

Finnerup, N.B., Sindrup, S.H., and Jensen, T.S. (2010). The evidence for pharmacological treatment of neuropathic pain. Pain 150, 573–581.

Friedman, A., Friedman, Y., Dremencov, E., and Yadid, G. (2008). VTA dopamine neuron bursting is altered in an animal model of depression and corrected by desipramine. J. Mol. Neurosci. 34, 201–209.

Friedman, A.K., Juarez, B., Ku, S.M., Zhang, H., Calizo, R.C., Walsh, J.J., Chaudhury, D., Zhang, S., Hawkins, A., Dietz, D.M., et al. (2016). KCNQ channel openers reverse depressive symptoms via an active resilience mechanism. Nat. Commun. 7, 11671.

Fu, B., Wen, S.N., Wang, B., Wang, K., Zhang, J.Y., Weng, X.C., and Liu, S.J. (2018). Gabapentin regulates dopaminergic neuron firing and theta oscillation in the ventral tegmental area to reverse depression-like behavior in chronic neuropathic pain state. J. Pain Res. 11, 2247–2256.

Gallagher, R.M., and Verma, S. (1999). Managing pain and comorbid depression: A public health challenge. Semin. Clin. Neuropsychiatry 4, 203–220.

Golden, S.A., Covington, H.E., III, Berton, O., and Russo, S.J. (2011). A standardized protocol for repeated social defeat stress in mice. Nat. Protoc. 6, 1183–1191.

Gonon, F.G. (1988). Nonlinear relationship between impulse flow and dopamine released by rat midbrain dopaminergic neurons as studied by in vivo electrochemistry. Neuroscience 24, 19–28.

Grace, A.A. (1991). Phasic versus tonic dopamine release and the modulation of dopamine system responsivity: a hypothesis for the etiology of schizophrenia. Neuroscience 41, 1–24.

Gunaydin, L.A., Grosenick, L., Finkelstein, J.C., Kauvar, I.V., Fenno, L.E., Adhikari, A., Lammel, S., Mirzabekov, J.J., Airan, R.D., Zalocusky, K.A., et al. (2014). Natural neural projection dynamics underlying social behavior. Cell 157, 1535–1551.

Hao, Y., Ge, H., Sun, M., and Gao, Y. (2019). Selecting an Appropriate Animal Model of Depression. Int. J. Mol. Sci. 20, 4827.

Hargreaves, K.M. (2011). Orofacial pain. Pain 152, S25–S32.

Hayashi, H., Iwata, M., Tsuchimori, N., and Matsumoto, T. (2014). Activation of peripheral KCNQ channels attenuates inflammatory pain. Mol. Pain 10, 15.

Hermanson, O., and Blomqvist, A. (1996). Subnuclear localization of FOS-like immunoreactivity in the rat parabrachial nucleus after nociceptive stimulation. J. Comp. Neurol. 368, 45–56.

Hermanson, O., and Blomqvist, A. (1997). Subnuclear localization of FOS-like immunoreactivity in the parabrachial nucleus after orofacial nociceptive stimulation of the awake rat. J. Comp. Neurol. 387, 114–123.

Huang, S., Borgland, S.L., and Zamponi, G.W. (2019). Peripheral nerve injury-induced alterations in VTA neuron firing properties. Mol. Brain 12, 89.

Huang, S., Zhang, Z., Gambeta, E., Xu, S.C., Thomas, C., Godfrey, N., Chen, L., M'Dahoma, S., Borgland, S.L., and Zamponi, G.W. (2020). Dopamine Inputs from the Ventral Tegmental Area into the Medial Prefrontal Cortex Modulate Neuropathic Pain-Associated Behaviors in Mice. Cell Rep. 31, 107812.

IsHak, W.W., Wen, R.Y., Naghdechi, L., Vanle, B., Dang, J., Knosp, M., Dascal, J., Marcia, L., Gohar, Y., Eskander, L., et al. (2018). Pain and Depression: A Systematic Review. Harv. Rev. Psychiatry 26, 352–363.

Krishnan, V., Han, M.H., Graham, D.L., Berton, O., Renthal, W., Russo, S.J., Laplant, Q., Graham, A., Lutter, M., Lagace, D.C., et al. (2007). Molecular adaptations underlying susceptibility and resistance to social defeat in brain reward regions. Cell 131, 391–404.

Lammel, S., Lim, B.K., Ran, C., Huang, K.W., Betley, M.J., Tye, K.M., Deisseroth, K., and Malenka, R.C. (2012). Input-specific control of reward and aversion in the ventral tegmental area. Nature 491, 212–217.

Lammel, S., Lim, B.K., and Malenka, R.C. (2014). Reward and aversion in a heterogeneous midbrain dopamine system. Neuropharmacology 76, 351–359.

Li, L., Sun, H., Ding, J., Niu, C., Su, M., Zhang, L., Li, Y., Wang, C., Gamper, N., Du, X., and Zhang, H. (2017). Selective targeting of M-type potassium K_v 7.4 channels demonstrates their key role in the regulation of dopaminergic neuronal excitability and depression-like behaviour. Br. J. Pharmacol. 174, 4277–4294.

Liu, M.Y., Yin, C.Y., Zhu, L.J., Zhu, X.H., Xu, C., Luo, C.X., Chen, H., Zhu, D.Y., and Zhou, Q.G. (2018). Sucrose preference test for measurement of stress-induced anhedonia in mice. Nat. Protoc. 13, 1686–1698.

Maeda, H., and Mogenson, G.J. (1982). Effects of peripheral stimulation on the activity of neurons in the ventral tegmental area, substantia nigra and midbrain reticular formation of rats. Brain Res. Bull. 8, 7–14.

Margolis, E.B., Toy, B., Himmels, P., Morales, M., and Fields, H.L. (2012). Identification of rat ventral tegmental area GABAergic neurons. PLoS One 7, e42365.

Obata, H. (2017). Analgesic Mechanisms of Antidepressants for Neuropathic Pain. Int. J. Mol. Sci. 18, 2483.

Ogawa, S.K., Cohen, J.Y., Hwang, D., Uchida, N., and Watabe-Uchida, M. (2014). Organization of monosynaptic inputs to the serotonin and dopamine neuromodulatory systems. Cell Rep. 8, 1105–1118.

Omelchenko, N., Bell, R., and Sesack, S.R. (2009). Lateral habenula projections to dopamine and GABA neurons in the rat ventral tegmental area. Eur. J. Neurosci. 30, 1239–1250.

Overton, P.G., and Clark, D. (1997). Burst firing in midbrain dopaminergic neurons. Brain Res. Brain Res. Rev. 25, 312–334.

Petit-Demouliere, B., Chenu, F., and Bourin, M. (2005). Forced swimming test in mice: a review of antidepressant activity. Psychopharmacology (Berl.) 177, 245–255.

Pradier, B., McCormick, S.J., Tsuda, A.C., Chen, R.W., Atkinson, A.L., Westrick, M.R., Buckholtz, C.L., and Kauer, J.A. (2019). Properties of neurons in the superficial laminae of trigeminal nucleus caudalis. Physiol. Rep. 7, e14112.

Rodriguez, E., Sakurai, K., Xu, J., Chen, Y., Toda, K., Zhao, S., Han, B.-X., Ryu, D., Yin, H., Liedtke, W., and Wang, F. (2017). A craniofacial-specific monosynaptic circuit enables heightened affective pain. Nat. Neurosci. 20, 1734–1743.

Schmidt, K., Forkmann, K., Schultz, H., Gratz, M., Bitz, A., Wiech, K., and Bingel, U. (2019). Enhanced Neural Reinstatement for Evoked Facial Pain Compared With Evoked Hand Pain. J. Pain 20, 1057–1069.

Sessle, B.J. (2000). Acute and chronic craniofacial pain: brainstem mechanisms of nociceptive transmission and neuroplasticity, and their clinical correlates. Crit. Rev. Oral Biol. Med. 11, 57–91.

Simon, G.E., VonKorff, M., Piccinelli, M., Fullerton, C., and Ormel, J. (1999). An international study of the relation between somatic symptoms and depression. N. Engl. J. Med. 341, 1329–1335.

Steru, L., Chermat, R., Thierry, B., and Simon, P. (1985). The tail suspension test: a new method for screening antidepressants in mice. Psychopharmacology (Berl.) 85, 367–370.

Sun, L., Liu, R., Guo, F., Wen, M.Q., Ma, X.L., Li, K.Y., Sun, H., Xu, C.L., Li, Y.Y., Wu, M.Y., et al. (2020). Parabrachial nucleus circuit governs neuropathic pain-like behavior. Nat. Commun. 11, 5974.

Suzuki, T., Morimoto, N., Akaike, A., and Osakada, F. (2020). Multiplex Neural Circuit Tracing With G-Deleted Rabies Viral Vectors. Front. Neural Circuits 13, 77.

Tan, A., Costi, S., Morris, L.S., Van Dam, N.T., Kautz, M., Whitton, A.E., Friedman, A.K., Collins, K.A., Ahle, G., Chadha, N., et al. (2020). Effects of the KCNQ channel opener ezogabine on functional connectivity of the ventral striatum and clinical symptoms in patients with major depressive disorder. Mol. Psychiatry 25, 1323–1333.

Tang, Y., Ma, L., Li, N., Guo, Y., Yang, L., Wu, B., Yue, J., Wang, Q., Liu, J., and Ni, J.X. (2016). Percutaneous trigeminal ganglion radiofrequency thermocoagulation alleviates anxiety and depression disorders in patients with classic trigeminal neuralgia: A cohort study. Medicine (Baltimore) 95, e5379.

Todd, A.J., Hughes, D.I., Polgár, E., Nagy, G.G., Mackie, M., Ottersen, O.P., and Maxwell, D.J. (2003). The expression of vesicular glutamate transporters VGLUT1 and VGLUT2 in neurochemically defined axonal populations in the rat spinal cord with emphasis on the dorsal horn. Eur. J. Neurosci. 17, 13–27.

Tye, K.M., Mirzabekov, J.J., Warden, M.R., Ferenczi, E.A., Tsai, H.C., Finkelstein, J., Kim, S.Y., Adhikari, A., Thompson, K.R., Andalman, A.S., et al. (2013). Dopamine neurons modulate neural encoding and expression of depression-related behaviour. Nature 493, 537–541.

Ungless, M.A., and Grace, A.A. (2012). Are you or aren't you? Challenges associated with physiologically identifying dopamine neurons. Trends Neurosci. 35, 422–430.

Vos, B.P., Strassman, A.M., and Maciewicz, R.J. (1994). Behavioral evidence of trigeminal neuropathic pain following chronic constriction injury to the rat's infraorbital nerve. J. Neurosci. 14, 2708–2723.

Watabe-Uchida, M., Zhu, L., Ogawa, S.K., Vamanrao, A., and Uchida, N. (2012). Whole-brain mapping of direct inputs to midbrain dopamine neurons. Neuron 74, 858–873.

Yadid, G., and Friedman, A. (2008). Dynamics of the dopaminergic system as a key component to the understanding of depression. Prog. Brain Res. 172, 265–286.

Yamada, M., Kawahara, Y., Kaneko, F., Kishikawa, Y., Sotogaku, N., Poppinga, W.J., Folgering, J.H., Dremencov, E., Kawahara, H., and Nishi, A. (2013). Upregulation of the dorsal raphe nucleus–prefrontal cortex serotonin system by chronic treatment with escitalopram in hyposerotonergic Wistar-Kyoto rats. Neuropharmacology 72, 169–178.

Yang, Y., Cui, Y., Sang, K., Dong, Y., Ni, Z., Ma, S., and Hu, H. (2018). Ketamine blocks bursting in the lateral habenula to rapidly relieve depression. Nature 554, 317–322.

Yang, H., de Jong, J.W., Cerniauskas, I., Peck, J.R., Lim, B.K., Gong, H., Fields, H.L., and Lammel, S. (2021). Pain modulates dopamine neurons via a spinal-parabrachial-mesencephalic circuit. Nat. Neurosci. 24, 1402–1413.

Zhang, H., Li, K., Chen, H.S., Gao, S.Q., Xia, Z.X., Zhang, J.T., Wang, F., and Chen, J.G. (2018). Dorsal raphe projection inhibits the excitatory inputs on lateral habenula and alleviates depressive behaviors in rats. Brain Struct. Funct. 223, 2243–2258.

Zhou, W., Jin, Y., Meng, Q., Zhu, X., Bai, T., Tian, Y., Mao, Y., Wang, L., Xie, W., Zhong, H., et al. (2019). A neural circuit for comorbid depressive symptoms in chronic pain. Nat. Neurosci. 22, 1649–1658.

Zweifel, L.S., Parker, J.G., Lobb, C.J., Rainwater, A., Wall, V.Z., Fadok, J.P., Darvas, M., Kim, M.J., Mizumori, S.J., Paladini, C.A., et al. (2009). Disruption of NMDAR-dependent burst firing by dopamine neurons provides selective assessment of phasic dopamine-dependent behavior. Proc. Natl. Acad. Sci. USA 106, 7281–7288.

STAR★METHODS

KEY RESOURCES TABLE

REAGENT or RESOURCE	SOURCE	IDENTIFIER
Antibodies		
anti-DAT	Abcam	184451; RRID: AB_2313773
anti-c-Fos	Abcam	190289; RRID: AB_2313773
anti-Vglut2	Abcam	79157; RRID: AB_2313773
Bacterial and virus strains		
rAAV-CAG-DIO-hChR2(H134R)-mCherry-WPREs-Pa	Hanbio Biotechnology	N/A
rAAV-CAG-DIO-NpHR-eYFP-WPREs-Pa	Hanbio Biotechnology	N/A
rAAV-CAG-DIO-mCherry-WPREs-Pa	Hanbio Biotechnology	N/A
rAAV-Ef1α-DIO-hM4D(Gi)/hM3D(Gq)-mCherry-WPREs-Pa	Hanbio Biotechnology	N/A
rAAV-Ef1α-DIO-mCherry-WPREs-Pa	Hanbio Biotechnology	N/A
rAAV-Ef1α-DIO-EGFP-WPRE-hGH-Pa	Hanbio Biotechnology	N/A
rAAV-Ef1α-DIO-RVG-WPRE-Pa	BrainVTA	N/A
rAAV-Ef1α-DIO-TVA-P2A-NLS-dTomato-WPRE-Pa	BrainVTA	N/A
RV-ENVA-ΔG-EGFP	BrainVTA	N/A
Chemicals, peptides, and recombinant proteins		
AP-5	Cayman Chemical	14539
Retigabine	Sigma	150812-12-7
Retrobeads	Lumafluor Inc	78R170
CNO	GLPBIO	GC10822
Experimental models: Organisms/strains		
C57BL/6J	The Jackson Laboratories	000664
DAT-Cre	The Jackson Laboratories	006660
Vglut2-Cre	The Jackson Laboratories	016963
Software and algorithms		
GraphPad Prism 8	GraphPad Software Inc.	https://www.graphpad.com
OriginPro 9.1	OriginLab Corporation	https://www.originlab.com/
Clampfit 10.3	Molecular Devices	https://www.moleculardevices.com/
BioRender	Created with BioRender.com	https://app.biorender.com/

RESOURCE AVAILABILITY

Lead contact

- Further information and requests for resources and reagents should be directed to and will be fulfilled by the lead contact, HZ (zhanghl@hebmu.edu.cn).

Materials availability

- This study did not generate new unique reagents.

Data and code availability

- Any additional information required to reanalyze the data reported in this paper is available from the lead contact upon request.
- Data reported in this paper will be shared by the lead contact upon request.
- This paper does not report original code.

EXPERIMENTAL MODEL AND SUBJECT DETAILS

The following mouse strain was used for this study: C57BL/6J – The Jackson Laboratories, Cat#: 000664; DAT-IRES-*cre* – The Jackson Laboratories, Cat#: 000664; Vglut2-ires-Cre – The Jackson Laboratories, Cat#: 000664. Male and female adult mice (6-10 weeks old) were used for all experiments. All procedures and experiments were approved by and done in accordance with the policies of Animal Care and Use Committee at Hebei Medical University and before and after any procedures, the mice were housed separately with access to water and food (provided by The Experimental Animal Center of Hebei Province) *ad libitum,* under controlled temperature (23–25 °C), humidity and lighting (12:12 h light–dark cycle). In all behavioral experiments, animals were allowed to adapt to the local environment for at least 1 day prior to experimentation. Male mice were used because of the social defeat depression model we used, as it is only suitable for male mice (Golden et al., 2011). Mice were housed separately to avoid aggressive behavior and to protect animals after the surgery or device implantation.

METHOD DETAILS

Animal models of neuropathic pain

Mice were anesthetized with pentobarbital sodium (50 mg/kg, i.p) before the pIONT (partial infraorbital nerve transection) operation. The infraorbital nerve, a branch of the trigeminal nerve emerging out of suborbital foramen and innervating the whisker pad, was exposed from the incision of the skin between eye and nose. A 1-2 mm segment of the nerve tract was ligated, transected and removed. The injury consists of both ligation and transection of most fibers in infraorbital nerve after passing through the foramen infraorbital[62]. After the operation, the skin was sutured and disinfected with iodophor.

Cannula implantation and intracerebral drug infusion

Mice were anesthetized with pentobarbital sodium (50 mg/kg, i.p), a stainless-steel cannula guide with double parallel pipeline (RWD Life Science, Shenzhen, China) was embedded into the ventral tegmental area (VTA) bilaterally (AP 3.08, LM ± 0.5, DP 4.2) using a brain stereotactic frame (RWD Life Science, Shenzhen, China) and was secured to the skull surface by dental cement. An injection cannula (0.2 mm protruded from the tip of the cannula guide, when plugged in) were connected to the cannula guide;a syringe (1 μl, Hamilton Company, USA) pre-filled with the injection solution was mounted to connect the injection cannula with an infusion pump (RWD Life Science, Shenzhen, China) set at a delivery rate of 100 nl/min (400 nL total volume). The intracranial infusion of a drug was initiated by plugging the injecting cannula into the cannula guide. Drugs were applied as follows: retigabine (200 μM), AP-5 (200 μM) and vehicle (artificial cerebrospinal fluid, ACSF), all in 400 nL total volume driven by an infusion pump at the rate 100 nL min^{-1}.

Viral injections

Mice were anesthetized with pentobarbital sodium (50 mg/kg, i.p) and fixed in the stereotactic frame. After drilling the hole into the skull surface, viral particles of 100-400 nL was injected into the target nuclei through a calibrated glass microelectrode connected to a syringe (1 μl, Hamilton Company, USA) using an infusion pump (RWD Life Science, Shenzhen, China) at the rate 50 nL min^{-1}. The specifics of the viral particles and purposes of the usage are explained below. The coordinates were defined as dorso-ventral (DV) from the brain surface, anterior–posterior (AP) from bregma and medio-lateral (ML) from the midline (in mm).

For retrograde tracing, the Cre-dependent virions rAAV-Ef1α-DIO-EGFP-WPRE-hGH-Pa (AAV2/9, 5.85×10^{12} vg ml^{-1}, 100 nl) were bilaterally injected into the VTA (AP, −3.08 mm; ML, ± 0.50 mm; DV, −4. 50 mm) and the LPBN (AP, −5.20 mm; ML, ± 1.25 mm; DV, −2.60 mm) of the Vglut2-Cre mice to confirm the projections PBL→VTA and Sp5C→PBL, respectively. For trans-monosynaptic retrograde tracing, first two types of viruses, rAAV-Ef1α-DIO-RVG-WPRE-Pa (AAV2/9, 5.29×10^{12} vg ml^{-1}, 150 nl) and rAAV-Ef1α-DIO-TVA-P2A-NLS-dTomato-WPRE-Pa (AAV2/9, 5.31×10^{12} vg ml^{-1}, 150 nl) were delivered to the PBL (AP, −5.20 mm; ML, ± 1.25 mm; DV, −2.60 mm) of the Vglut2-Cre mice acting as helpers. After 3 weeks, modified rabies virus RV-ENVA-ΔG-EGFP ($\geq 2.00 \times 10^8$ IFU ml^{-1}, 200nl) was injected into VTA (AP, −3.08 mm; ML, ± 0.50 mm; DV, −4. 50 mm) to specifically infect the terminals of PBL→VTA neurons, due to the expression of TVA. Combined with rabies glycoprotein, *trans*-synaptic retrograde labeling was achieved in Sp5C→PBL→VTA.

For optogenetics, rAAV-CAG-DIO-hChR2(H134R)-mCherry-WPREs-Pa (AAV2/9, 1.20×10^{12} vg ml^{-1}, 300 nl) or rAAV-CAG-DIO-NpHR-eYFP-WPREs-Pa (AAV2/9, 1.20×10^{12} vg ml^{-1}, 300 nl) were delivered into the VTA (AP, −3.08 mm; ML, −0.50 mm; DV, −4. 50 mm), the LPBN (AP, −5.20 mm; ML, −1.25 mm; DV, −2.60 mm) and the Sp5C (AP, −6.60 mm; ML, −1.75 mm; DV, −3.50 mm) of the respective mice used. The control construct for these injections was rAAV-CAG-DIO-mCherry-WPREs-Pa (AAV2/9, 1.20×10^{12} vg ml^{-1}, 300 nl). The optic fibers were implanted to the VTA (AP, −3.08 mm; ML, −0.50 mm; DV, −4. 50 mm) and LPBN (AP, −5.20 mm; ML, −1.25 mm; DV, −2.60 mm).

For chemogenetics, rAAV-Ef1α-DIO-hM4D(Gi)/hM3D(Gq)-mCherry-WPREs-Pa (AAV2/9, 2.00×10^{12} vg ml^{-1}, 300 nl) or its control rAAV-Ef1α-DIO-mCherry-WPREs-Pa (AAV2/9, 2.00×10^{12} vg ml^{-1}, 300 nl) were delivered into the VTA (AP, −3.08 mm; ML, ± 0.50 mm; DV, −4. 50 mm) of the mice used.

All the above viruses were provided by The BrainVTA (Wuhan, China).

Neuron projection tracing

Retrobeads (Lumafluor Inc, USA) were used for projection tracing. The injection procedures were same as for the viral injections described above. For LPBN-VTA tracing, retrobeads (100 nl) were injected into the VTA (AP, −3.08 mm; ML, ± 0.50 mm; DV, −4.50 mm). For Sp5C-LPBN tracing, retrobeads (100 nl) were injected into the LPBN (AP, −5.20 mm; ML, ± 1.25 mm; DV, −2.60 mm). The retrobeads and the fluorescence proteins (GFP, mCherry) carried by the viruses were visualized in the brain sections by confocal microscopy using Nikon A1 (Nikon, Japan). For the brain-wide imaging, the coronal brain sections were cut at 30 μm thickness every 200 μm of midbrain and hindbrain using a vibratome (VT1200S; Leica, Germany).

Optogenetics

Five minutes after virus injection, an optical fiber was implanted into the VTA (AP, −3.08 mm; ML, −0.50 mm; DV, −4.50 mm) and the LPBN (AP, −5.20 mm; ML, −1.25 mm; DV, −2.60 mm) at the 21st day after surgery following virus injection and the fiber was fixed with dental cement to the skull. The fiber was connected to a laser source (Changchun New Industries Optoelectronics Technology, China) emitting blue (475 nm, 1.5 mW, 20 Hz, 5 pulses, interval 10 s) or yellow (590 nm, 5–8 mW, constant) light.

Chemogenetics

One week after the injection of AAV-DIO-hM4D(Gi)-mCherry/AAV-DIO-hM3D-mCherry or AAV-DIO-mCherry and before the behavioral tests, clozapine N-oxide, CNO (3.3 mg kg^{-1}, i.p.) was scheduled 15 minutes prior to the test.

Electrophysiology

Single-unit recording and local pressure drug administration

Single-unit recordings were used to record the spontaneous firing of the VTA dopaminergic (DA) neurons *in vivo*. Mice were anesthetized by pentobarbital sodium (50 mg/kg, i.p), fixed to the stereotactic frame and spontaneous firing was recorded in the VTA (AP, −3.04 ± 0.12 mm; ML, 0.50 ± 0.10 mm; DV, −4.60 ± 0.40 mm). DA neurons were identified by their characteristic action potentials: typically triphasic action potentials with a negative deflection: the action potential width from the start to the minimum of ≥ 1.1 ms, a characteristic long duration (> 2 ms) and a slow firing rate (< 10 Hz) (Ungless and Grace, 2012). It should be noted that characteristics of action potential is not always a reliable way to differentiate the DA neurons from the GABA neurons (Margolis et al., 2012). The presence of burst firing (as opposed to tonic firing) was identified by the following criteria: (i) the start of a burst was registered when two consecutive spikes fired within 80 ms; (ii) the end of the burst was registered when the interspike interval (ISI) exceeded 160 ms; and (iii) a neuron was considered as burst-firing if it fired at least one burst within 3 min. Electrical signals were amplified and filtered by the Axoclamp 900A preamplifier and recorded by the Digidata 1440A AD converter (Molecular Devices, USA); the data were analyzed by Clampfit 10.3 (Molecular Devices, USA).

The effect of Retigabine (200 μM), AP-5 (200 μM) and ACSF (vehicle) on the firing activity of the VTA DA neurons recorded using the single-unit method was assessed 5 min after direct VTA local pressure (5–15 ψ) administration (PDES-02DX, NPI Electronic, Germany). The effects of drugs were analyzed on the following parameters: (i) average firing rates (Hz); (ii) average number of bursts per minute; (iii) average number of spikes in a burst.

Brain slice preparation and cell-attached patch clamp recording

Mice were anesthetized with pentobarbital sodium (100 mg/kg, i.p) and perfused intracardially with ice-cold sucrose solution (in mM: 260 sucrose, 3 KCl, 26 NaHCO$_3$, 1.25 NaH$_2$PO$_4$, 2 CaCl$_2$, 2 MgCl$_2$, 10 D-glucose, saturated with 95% O$_2$/5% CO$_2$). Coronal midbrain slices (200 μm) containing the VTA were cut by a vibratome (VT1200S; Leica, Germany) in ice-cold sucrose solution and then placed in 37°C oxygenated ACSF (in mM: 130 NaCl, 3 KCl, 26 NaHCO$_3$, 1.25 NaH$_2$PO$_4$, 2 CaCl$_2$, 2 MgCl$_2$, 10 D-glucose) for 30 min. The slices were then left to recover at room temperature for about 90 min, transferred to the recording chamber and perfused with oxygenated ACSF. Patch pipettes (3–5 MΩ, pulled from borosilicate glass capillaries by a four-stage horizontal puller, P97, Sutter Instruments, USA) were filled with ACSF. The spontaneous firing activity was recorded in the cell-attached mode; electrical signals were amplified and filtered by the Axoclamp 700B preamplifier and recorded by the Digidata 1440A AD converter (Molecular Devices, USA); the data were analyzed by Clampfit 10.3 (Molecular Devices, USA).

Immunohistochemistry

Mice were anesthetized with pentobarbital sodium (100 mg/kg, i.p) and intracardially perfused with 20 mL cold PBS containing PFA (4%). The brains were removed and post-fixed in PFA (4%) at 4°C overnight and transferred into 30% sucrose solution at 4°C for 48 hours dehydration. The tissue was then sectioned into coronal sections (40 μm thick) using a vibratome (Leica VT1200s, Germany). The sections were incubated in blocking buffer (3% BSA, PBS with 0.3% Triton X-100) containing 10% donkey serum for 1 h at room temperature, and then incubated with primary antibodies, including anti-DAT (1:500, rabbit, Abcam), anti-c-Fos (1:400, mouse, Abcam), anti-Vglut2 (1:500, mouse, Abcam) at 4 °C for 24 h, followed by the incubation with the corresponding fluorophore-conjugated secondary antibodies (Jackson ImmunoResearch, USA) for 1 h at room temperature. Images were acquired using a Leica TCS SP5 confocal laser microscope (Leica, Germany) or Nikon A1 (Nikon, Japan) equipped with laser lines for 405 mm, 488 mm, 561 mm and 647 mm illumination.

Behavioral assessment of neuropathic pain and depressive-like behavior

Mice for testing were transferred to the testing room 24 h before the test for accommodation. During the testing session, the behavior of the animals was recorded using a video tracking system and was subsequently analyzed offline. The experimenter was blinded to group identity during the experiment and quantitative analyses.

Face-grooming

A mouse was placed into a translucent enclosure and left for 1 hour to adapt. Face-grooming actions were counted over a period of 2 min and quantified as frequency (strokes/min). The identification of face-grooming actions was judged by the position of the paw over the facial region, following the method described in detail (Berridge, 1990).

Tail suspending test, TST

Mice were suspended by the tail using an adhesive tape at 1 cm from the tip of the tail sticking to a bar 50 cm above the plane. Each mouse was tested only once for 6 min. The test was videotaped from the side and the immobility time of the animal was measured in the last 4 min of the test. Immobility was considered as a period of time without initiated movements, including passive swaying (Steru et al., 1985).

Forced swimming test, FST

Mice were individually placed in a cylindrical container (12 cm diameter, 25 cm height) of 24 °C water for 6 min. Mice swam for 6 min under normal light and were videotaped from the side. The immobility time during the last 4 min of the test was counted. Immobility was defined as time when animals remained floating or motionless with only movements necessary for keeping balance in the water (Petit-Demouliere et al., 2005).

Sucrose preference test, SPT

Sucrose solution (1%) or drinking water was filled in 50 mL bottles with stoppers. All animals were singly housed and acclimatized to two-bottle choice conditions for 12 h. After this, the positions of the tubes were interchanged and animals were left for further 12 h, at the end of experiment fluid in both bottles was weighed.

Open filed test, OFT

Exploration of an open field arena (50 × 50 cm) was assessed during a 30-min test. A video-tracking system (Harvard Bioscience (Shanghai) Co., Ltd., China) measured locomotor activity, as well as the time spent in the center (40 × 40 cm) and corners of the test arena. The area was cleaned with 75% ethanol after each test to remove olfactory cues from the apparatus.

Mechanical and thermal sensitivity (hind paw)

Mechanical withdrawal threshold was measured by using Von Frey filaments (Stoelting Co, Chicago, IL, USA). Each mouse was placed into a plastic cage with a wire mesh bottom. A single filament was applied perpendicularly to the plantar surface of the hind paw for five times with an interval of 5 s. Positive response was defined as three clear withdrawal responses out of five applications. Filaments were applied in an up-and-down order according to a negative or positive response to determine the hind paw withdrawal threshold.

Thermal withdrawal latency (Hargreaves method) in response to radiant heat (PL-200, Taimeng Co, Chengdu, China) was used to evaluate thermal sensitivity. The intensity of the radiant heat stimulus was maintained at 15%. Mice were placed individually into plexiglass cubicles placed on a transparent glass surface. The light beam from radiant heat lamp, located below the glass, was directed at the plantar surface of hindpaw. The time from the onset of radiant heat stimulation to withdrawal of the hindpaw (elapsed time) was recorded. Three trials with an interval of 5 min were made for each mouse, and scores from three trials were averaged.

The subthreshold social-defeat and social-interaction test

The subthreshold social-defeat paradigm involved placing the test C57BL/6J mouse into the home cage of a larger retired breeder mouse (CD1) for 2 min during which time the experimental mouse was physically attacked by the CD1 mouse. After two bouts of defeat the mouse was returned to its home cage. Mice underwent the social-interaction test 24 h after the defeat episodes.

The social interaction test (Golden et al., 2011), measured the time spent in the interaction zone, corner zones and locomotor activity during the first (CD1 target absent in interaction zone) and second (CD1 target present in interaction zone) trials in an open-field arena. Mouse movements were automatically monitored and recorded (Smart 3.0, Panlab, S.L.U, Spain) for 2.5 min per each test session. Behavioral phenotype was based on the social interaction ratio, which was calculated as as a ratio of the time spent in the interaction and corner zone with target present divided by the time spent in the interaction and corner zone with the target absent. All mice with an interaction ratio above 1 and corner ratio below 1 were classified as normal, and all mice with an interaction ratio below 1 and corner ratio above 1 were classified as being having depression-like behavior.

cFos immunofluorescence

Quantification of cFos expression was performed by counting neurons with mean fluorescence intensity at least 3 times above the background fluorescence intensity (mean fluorescence intensity of an area without visible neurons). For a quantitative comparison, we denoted the difference in the numbers of cFos-positive cells in a given brain area of pIONT versus sham mice as follows: *20-50 neurons difference; **50-200 neurons difference; *** > 200 neurons difference

QUANTIFICATION AND STATISTICAL ANALYSIS

All data are expressed as the mean ± s.e.m. Paired-samples t test was used to compare the means of two groups when the data were normally distributed. Multiple groups were compared using One-way ANOVA with Bonferroni correction. Pharmacological effects on the behavioral test were analyzed using repeated-measures ANOVA with Bonferroni correction. An unpaired t test was used to compare the behavior and electrophysiological results between the pIONT and sham groups. For data that failed the normality test, the paired sample Wilcoxon signed rank test or Mann-Whitney tests were used. Significance levels were indicated as $*p < 0.05$, $**p < 0.01$ and $***p < 0.001$. GraphPad Prism 8 (GraphPad Software Inc., San Diego, CA, USA), OriginPro 9.1 software (OriginLab Corporation, USA) and illustrator (Adobe Systems Incorporated, USA) were used for the statistical analyses and graphing.